

Lepton Flavour Violation in Hadron Decays of the Tau Lepton within the Littlest Higgs Model with T-parity

Iván Pacheco and Pablo Roig

Departamento de Física, Centro de Investigación y de Estudios Avanzados del Instituto Politécnico Nacional

Apartado Postal 14-740, 07000 Ciudad de México, México

E-mail: ipacheco@fis.cinvestav.mx, proig@fis.cinvestav.mx

ABSTRACT: We first study the hadronic lepton flavor violating tau decays within the littlest Higgs model with T-parity (including one or two pseudoscalars, or a vector resonance). We consider the case where only T-odd particles and partner fermions contribute, and also its extension including Majorana neutrinos coming from an inverse seesaw. In both cases our mean values lie only one order of magnitude below current upper limits, strengthening the case of searching for these decays in the quest for new physics.

Contents

| | | |
|----------|---|-----------|
| 1 | Introduction | 2 |
| 2 | Littlest Higgs model with T parity (LHT) | 3 |
| 3 | Inverse seesaw neutrino masses in the LHT model | 4 |
| 4 | Lepton Flavour Violating Hadron Decays of the Tau Lepton | 5 |
| 4.1 | $\tau \rightarrow \ell q \bar{q}$ ($\ell = e, \mu$) | 5 |
| 4.1.1 | T-odd contribution | 6 |
| 4.1.2 | Majorana contribution | 9 |
| 4.2 | Hadronization | 12 |
| 4.3 | $\tau \rightarrow \ell P$ ($\ell = e, \mu$) | 14 |
| 4.3.1 | $\tau \rightarrow \mu \pi^0$ | 14 |
| 4.3.2 | $\tau \rightarrow \mu \eta$ | 15 |
| 4.3.3 | $\tau \rightarrow \mu \eta'$ | 16 |
| 4.4 | $\tau \rightarrow \ell PP$ ($\ell = e, \mu$) | 17 |
| 4.4.1 | $\tau \rightarrow \mu \pi^+ \pi^-$ | 17 |
| 4.4.2 | $\tau \rightarrow \mu K^+ K^-$ | 17 |
| 4.4.3 | $\tau \rightarrow \mu K^0 \bar{K}^0$ | 18 |
| 4.5 | $\tau \rightarrow \ell V$ ($\ell = e, \mu, V = \rho, \phi$) | 18 |
| 5 | Phenomenology | 19 |
| 5.1 | $\tau \rightarrow \ell P$ ($\ell = e, \mu$) | 20 |
| 5.2 | $\tau \rightarrow \ell PP, \ell V$ ($\ell = e, \mu$) | 25 |
| 6 | Conclusions | 34 |
| A | Appendix: Form Factor Functions of T-odd Contribution | 35 |
| B | Appendix: Form Factor Functions of Majorana Contribution | 36 |
| C | Appendix: Hadronization tools | 38 |
| C.1 | $\tau \rightarrow \mu P$ | 39 |
| C.2 | $\tau \rightarrow \mu PP$ | 40 |
| C.3 | $\tau \rightarrow \mu V$ | 41 |
| D | Appendix: Hadronic form factors | 41 |

1 Introduction

A scalar boson mass is not protected by any symmetry, unlike the case of spin 1/2 fermions and spin 1 bosons. For them, chiral and gauge symmetries, respectively, ensure that the quantum corrections to their masses vanish in the limit of small bare masses. The presence of a Higgs boson [1–4] with mass on the electroweak scale ($\sim v$) [5, 6] is unnatural upon the existence of heavy new particles coupling to it proportionally to their masses. This was christened as the hierarchy problem [7], whose solution is still unknown. The fact that the Standard Model (SM) [8–10] is incomplete ¹, together with the strong restrictions on new physics close to v coming from very accurate low-energy measurements, electroweak precision data and LHC constraints [11], aggravates the hierarchy issue. Famous solutions to it include supersymmetry or extra dimensions, and little Higgs models, to which our work belongs.

Composite Higgs models [12–15] update the ideas of technicolor [16]. Thus, the Higgs boson is a pseudo-Nambu-Goldstone boson of a spontaneously broken global symmetry at a scale $f > v$. As a result, the Higgs mass is of $\mathcal{O}(v)$ despite the existence of new physics at the scale f . In this way the hierarchy problem is not solved but delayed up to the energy where the model becomes strongly coupled. Specifically, we will work within the Littlest Higgs model with T-parity (LHT) [12, 17–22], whose fermion sector is reviewed in section 2. The spontaneous collective breaking of the LHT corresponds to a global symmetry group $SU(5)$ broken down to $SO(5)$, by a vacuum expectation value at the TeV scale. Discrete T parity symmetry is imposed to avoid singly-produced new heavy particles and tree level corrections to SM observables. Thus, LHT is not stringently constrained by data [23, 24]. Varied aspects of its phenomenology have been studied in refs. [23–39], in particular lepton flavor violating processes have been analyzed in refs. [32, 40–51].

LHT possibly realizing a low-scale seesaw and in particular one of inverse type (ISS) was put forward recently in ref. [51]. In our previous article [52], we showed that purely leptonic LFV processes and $\mu \rightarrow e$ conversion in nuclei were closer to current bounds within this setting than in the standard LHT (see e.g. ref. [50]). These results motivated us to analyze semileptonic LFV tau decays in this work. Although they are quite suppressed in the Simplest Little Higgs model (SLH) [53], the richer composition of the LHT (even in absence of additional Majorana neutrinos coming from the ISS) should enable larger rates than in the SLH. We will show that branching ratios within one order of magnitude of current upper limits can be expected in the processes studied in this work.

This article is structured as follows: after a brief review of the fermion sector of the LHT in section 2, we summarize the realization of the ISS within the LHT in section 3. Then, in section 4 we present the different contributions to the considered semileptonic LFV tau decays. We start with the parton process in section 4.1 and continue -accounting for the corresponding hadronization- with the decays including one meson (section 4.3), two mesons (section 4.4) and one vector resonance (section 4.5). Associated phenomenology is discussed in section 5 (first in the standard LHT and then adding Majorana neutrino contributions, arising from the ISS) and our conclusions are given in section 6. Appendices

¹At least it lacks a mechanism to generate the observed baryon asymmetry of the universe.

include form factors for T -odd (appendix A) and Majorana (appendix B) contributions as well as a survey on hadronization techniques (appendix C) and corresponding form factors (appendix D).

2 Littlest Higgs model with T parity (LHT)

We develop here just the fermion sector to illustrate what are the new particles in the LHT and how they acquire mass. We embed two $SU(5)$ incomplete quintuplets and introduce a right-handed $SO(5)$ multiplet Ψ_R [54]

$$\Psi_1 = \begin{pmatrix} i\psi_1 \\ 0 \\ 0 \end{pmatrix}, \quad \Psi_2 = \begin{pmatrix} 0 \\ 0 \\ i\psi_2 \end{pmatrix}, \quad \Psi_R = \begin{pmatrix} \psi_R^c \\ \chi_R \\ \psi_R \end{pmatrix}, \quad (2.1)$$

where the superscript $(^c)$ denotes a partner lepton field, not to be confused with charge conjugation, and χ_R is a lepton singlet (see section 3). Above (σ^2 is the second Pauli matrix)

$$\psi_i = -\sigma^2 \begin{pmatrix} \nu_{L_i} \\ \ell_{L_i} \end{pmatrix} \quad (i = 1, 2), \quad \psi_R = -\sigma^2 \begin{pmatrix} \nu_{HR} \\ \ell_{HR} \end{pmatrix}. \quad (2.2)$$

The action of T-parity on the LH leptons is then defined to be

$$\Psi_1 \longleftrightarrow \Omega \Sigma_0 \Psi_2, \quad (2.3)$$

with

$$\Omega = \text{diag}(-1, -1, 1, -1, -1), \quad \Sigma_0 = \begin{pmatrix} 0 & 0 & \mathbf{1}_{2 \times 2} \\ 0 & 1 & 0 \\ \mathbf{1}_{2 \times 2} & 0 & 0 \end{pmatrix}. \quad (2.4)$$

This discrete symmetry is implemented in the fermion sector duplicating the SM doublet $l_L = (l_{1L} - l_{2L})/\sqrt{2}$, corresponding to the T-even combination $(\Psi_1 + \Omega \Sigma_0 \Psi_2)/\sqrt{2}$, that remains light, with an extra heavy mirror doublet $l_{HL} = (\nu_{HL}, \ell_{HL})^T = (l_{1L} + l_{2L})/\sqrt{2}$ obtained from the T-odd orthogonal combination $(\Psi_1 - \Omega \Sigma_0 \Psi_2)/\sqrt{2}$. The mirror leptons can be given $\mathcal{O}(f)$ masses via [55]

$$\mathcal{L}_{Y_H} = -\kappa f \left(\bar{\Psi}_2 \xi + \bar{\Psi}_1 \Sigma_0 \xi^\dagger \right) \Psi_R + h.c., \quad (2.5)$$

where $\xi = e^{i\Pi/f}$ and f is the new physics (NP) energy scale of $\mathcal{O}(\text{TeV})$. For $\xi = \exp(i\Pi/f) \approx \mathbb{I}$, this Lagrangian gives a vector-like mass $\sqrt{2}\kappa f$ to ν_H . The mirror leptons thus acquire masses after EWSB, given by [54, 56]

$$m_{\ell_H^i} = \sqrt{2}\kappa_{ii}f \equiv m_{Hi}, \quad m_{\nu_H^i} = m_{Hi} \left(1 - \frac{v^2}{8f^2} \right), \quad (2.6)$$

where κ_{ii} are the eigenvalues of the mass matrix κ . Partner leptons $\bar{\ell}^c = (\bar{\nu}^c, \bar{\ell}^c)$ also appear. To give them masses we need to introduce another $SO(5)$ multiplet [57, 58]

$$\tilde{\Psi}_R = \begin{pmatrix} 0 \\ \tilde{\chi}_R \\ \tilde{\psi}_R \end{pmatrix}, \quad \tilde{\Psi}_R \xrightarrow{T} -\tilde{\Psi}_R. \quad (2.7)$$

This multiplet introduces Dirac mass terms for the ψ_R^c and χ_R fields as follows

$$\mathcal{L}_{Y_H} = -\kappa f \left(\bar{\Psi}_2 \xi + \bar{\Psi}_1 \Sigma_0 \xi^\dagger \right) \Psi_R + \kappa_2 \tilde{\Psi}_R^T \Psi_R + \text{h.c.} \quad (2.8)$$

Thus, partner leptons receive a κ_2 mass.

It happens similarly for the masses of T-odd quarks, with κ_{ii}^q instead of κ_{ii} , and replacing d_H -quark by ℓ_H , u_H -quark by ν_H and κ_2^q by κ_2 for the mass matrix of partner quarks of u and d types.

3 Inverse seesaw neutrino masses in the LHT model

The lepton singlets χ_R also get a large (vector-like) mass by combining with a LH singlet χ_L through a direct mass term without further couplings to the Higgs. Therefore, its mass term is written

$$\mathcal{L}_M = -M \bar{\chi}_L \chi_R + \text{h.c.} \quad (3.1)$$

We stress that χ_L is an $SU(5)$ singlet. Consequently, it is natural to include a small Majorana mass for it. Once lepton number is assumed to be only broken by small Majorana masses μ in the heavy LH neutral sector,

$$\mathcal{L}_\mu = -\frac{\mu}{2} \bar{\chi}_L^c \chi_L + \text{h.c.}, \quad (3.2)$$

so the resulting (T-even) neutrino mass matrix reduces to the inverse see-saw one [55]

$$\mathcal{L}_M^\nu = -\frac{1}{2} \left(\bar{\nu}_l^c \quad \bar{\chi}_R^c \quad \bar{\chi}_L^c \right) \mathcal{M}_\nu^{T\text{-even}} \begin{pmatrix} \nu_L \\ \chi_R^c \\ \chi_L \end{pmatrix} + \text{h.c.}, \quad (3.3)$$

where

$$\mathcal{M}_\nu^{T\text{-even}} = \begin{pmatrix} 0 & i\kappa^* f \sin\left(\frac{v}{\sqrt{2}f}\right) & 0 \\ i\kappa^\dagger f \sin\left(\frac{v}{\sqrt{2}f}\right) & 0 & M^\dagger \\ 0 & M^* & \mu \end{pmatrix}, \quad (3.4)$$

with each entry standing for a 3×3 matrix to take into account the 3 lepton families. The κ entries are given by the Yukawa Lagrangian in eq. (2.8) and M stands for the direct heavy Dirac mass matrix from eq. (3.1). Finally, μ is the mass matrix of small Majorana masses in eq. (3.2).

Upon considering the hierarchy $\mu \ll \kappa \ll M$ (inverse see-saw), the mass eigenvalues for M are ~ 10 TeV, of the order of $4\pi f$ with $f \sim TeV$, as required by current EWPd if we assume the κ eigenvalues to be order 1 [52]. Conversely, the μ eigenvalues shall be much smaller than the GeV.

After diagonalizing the mass matrix from eq.(3.4), in the mass eigenstates basis, the SM charged and neutral currents become [52]

$$\begin{aligned} \mathcal{L}_W^l &= \frac{g}{\sqrt{2}} W_\mu^+ \sum_{i,j=1}^3 \bar{\nu}_i^l W_{ij} \gamma^\mu P_L \ell_j + \text{h.c.}, \quad \text{with} \quad W_{ij} = \sum_{k=1}^3 U_{ik}^\dagger \left[\mathbf{1}_{3 \times 3} - \frac{1}{2}(\theta\theta^\dagger) \right]_{kj}, \\ \mathcal{L}_W^{lh} &= \frac{g}{\sqrt{2}} W_\mu^+ \sum_{i,j=1}^3 \bar{\chi}_i^h \theta_{ij}^\dagger \gamma^\mu P_L \ell_j + \text{h.c.} \end{aligned} \quad (3.5)$$

and

$$\begin{aligned}
\mathcal{L}_Z^l &= \frac{g}{2 \cos \theta_W} Z_\mu \sum_{i,j=1}^3 \bar{\nu}_i^l \gamma^\mu (X_{ij} P_L - X_{ij}^\dagger P_R) \nu_j^l, \quad \text{with} \quad X_{ij} = \sum_{k=1}^3 \left(U^\dagger [\mathbf{1}_{3 \times 3} - (\theta \theta^\dagger)] \right)_{ik} U_{kj}, \\
\mathcal{L}_Z^{lh} &= \frac{g}{2 \cos \theta_W} Z_\mu \sum_{i,j=1}^3 \bar{\chi}_i^h \gamma^\mu (Y_{ij} P_L - Y_{ij}^\dagger P_R) \nu_j^l + h.c., \quad \text{with} \quad Y_{ij} = \sum_{k=1}^3 \theta_{ik}^\dagger U_{kj}, \\
\mathcal{L}_Z^h &= \frac{g}{2 \cos \theta_W} Z_\mu \sum_{i,j=1}^3 \bar{\chi}_i^h \gamma^\mu (S_{ij} P_L - S_{ij}^\dagger P_R) \chi_j^h, \quad \text{with} \quad S_{ij} = \sum_{k=1}^3 \theta_{ik}^\dagger \theta_{kj},
\end{aligned} \tag{3.6}$$

where θ matrix elements give the mixing between light and heavy (quasi-Dirac) neutrinos to leading order, and $U = U_{PMNS}$.

Assuming universality and, in particular, that the three mixing angles θ_{ii} are equal, their absolute value is found to be < 0.03 at 95% C.L. [59]. Hence,

$$|\kappa_{ii}| < 0.17 \left(\frac{M_i}{\text{TeV}} \right) \leq 2.136 \left(\frac{f}{\text{TeV}} \right), \tag{3.7}$$

for $f > 1$ TeV. This effective description requires $M_i \lesssim 4\pi f$, with M_i the heavy Majorana neutrino masses.

4 Lepton Flavour Violating Hadron Decays of the Tau Lepton

In this section we apply our model for the study of LFV tau decays into hadrons: $\tau \rightarrow \mu P$, $\tau \rightarrow \mu V$ and $\tau \rightarrow \mu P \bar{P}$ where P (V) is short for a pseudoscalar (vector) meson². For the single meson case, we will consider $P = \pi^0, \eta, \eta'$. For the two-meson channels, we will restrict ourselves to the numerically leading $P = \pi, K$ cases. Correspondingly, $V = \rho, \phi$ (ω being suppressed).

We are going to consider the effects of T-odd and partner particles as well as heavy Majorana neutrinos since terms of order $\mathcal{O}(v^2/f^2)$ are taken into account, where v is the vev of the SM Higgs and f is the energy scale of NP ($\sim \text{TeV}$), such that $v^2/f^2 \ll 1$. We begin our analysis determining the amplitudes of the $\tau \rightarrow \mu q \bar{q}$ process, with $q = u, d, s$ quarks and, afterwards, proceed to hadronize the corresponding quarks bilinears. For this latter step we will employ the tools given by chiral symmetry and dispersion relations, enforcing the right short-distance behaviour to the form factors.

4.1 $\tau \rightarrow \ell q \bar{q}$ ($\ell = e, \mu$)

Two generic topologies are involved in this amplitude: i) penguin-like diagrams, namely $\tau \rightarrow \ell \{\gamma, Z\}$, followed by $\{\gamma, Z\} \rightarrow q \bar{q}$ and ii) box diagrams. We will assume, for simplicity, that light quarks and leptons (ℓ) are massless in our calculation. Corrections induced by their finite masses can be safely neglected.

²Effective field theory analyses of these processes can be found in refs. [60–63].

The full amplitude is given by two contributions: one of them comes from T-odd particles and the other from heavy Majorana neutrinos, then

$$\mathcal{M} = \mathcal{M}^{\text{T-odd}} + \mathcal{M}^{\text{Maj}}, \quad (4.1)$$

where each one is written

$$\begin{aligned} \mathcal{M}^{\text{T-odd}} &= \mathcal{M}_\gamma^{\text{T-odd}} + \mathcal{M}_Z^{\text{T-odd}} + \mathcal{M}_{\text{box}}^{\text{T-odd}}, \\ \mathcal{M}^{\text{Maj}} &= \mathcal{M}_\gamma^{\text{Maj}} + \mathcal{M}_Z^{\text{Maj}} + \mathcal{M}_{\text{box}}^{\text{Maj}}, \end{aligned} \quad (4.2)$$

we will use the 't Hooft-Feynman gauge along the calculation and will write $\ell = \mu$ for definiteness.

4.1.1 T-odd contribution

The Feynman diagrams that contribute to the $\mathcal{M}_\gamma^{\text{T-odd}}$ amplitude are shown in Figure 1, whose structure follows

$$\mathcal{M}_\gamma^{\text{T-odd}} = \frac{e^2}{Q^2} \bar{\mu}(p') [2iF_M^\gamma(Q^2) P_R \sigma^{\mu\nu} Q_\nu + F_L^\gamma(Q^2) \gamma^\mu P_L] \tau(p) \bar{q}(p_q) Q_q \gamma_\mu q(p_{\bar{q}}), \quad (4.3)$$

where $Q^2 = (p_q + p_{\bar{q}})^2$ is the squared momentum transfer and F_M^γ is given by ³

$$F_M^\gamma = F_M^\gamma|_{W_H} + F_M^\gamma|_{Z_H} + F_M^\gamma|_{A_H} + F_M^\gamma|_{\bar{\nu}^c} + F_M^\gamma|_{\bar{\ell}^c}. \quad (4.4)$$

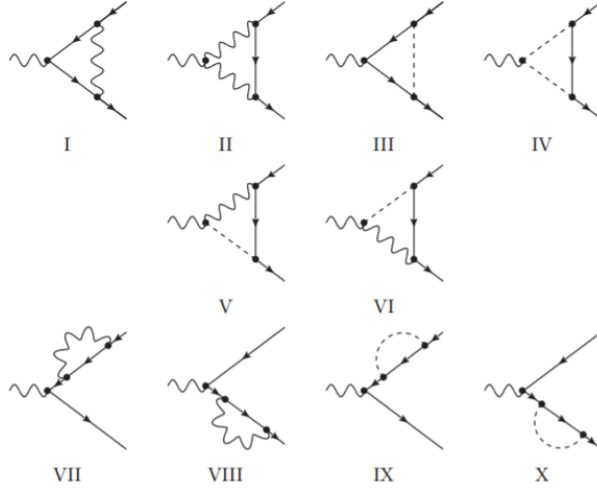


Figure 1. Topologies of the diagrams that contribute to the processes $\gamma, Z \rightarrow \bar{\ell}\ell'$.

³Within the LHT, there appear new heavy gauge bosons and a scalar electroweak triplet with $\mathcal{O}(f)$ masses: A_H, Z_H, W_H, Φ , see eq. (5.1). The corresponding Goldstone bosons of the former come from the Π matrix [41, 50], see eq. (2.5) and text below.

In this case we consider terms of order $\mathcal{O}(Q^2)$. All functions below agree with ref. [50]. We write explicitly the above form factor

$$F_M^\gamma = \frac{\alpha_W}{16\pi} \frac{m_\tau}{M_W^2} \frac{v^2}{4f^2} \sum_i V_{H\ell}^{i\mu\dagger} V_{H\ell}^{i\tau} \left[F_{W_H}(y_i, Q^2) + F_{Z_H}(y_i, Q^2) + \frac{1}{5} F_{Z_H}(ay_i, Q^2) \right] \\ + \frac{\alpha_W}{16\pi} \frac{m_\tau}{M_\Phi^2} \frac{v^2}{4f^2} \sum_{i,j,k} V_{H\ell}^{i\mu\dagger} \frac{m_{\ell_{Hi}}}{M_W} W_{ij}^\dagger W_{jk} \frac{m_{\ell_{Hk}}}{M_W} V_{H\ell}^{k\tau} [F_{\bar{\nu}^c}(x_j, Q^2) + F_{\bar{\ell}^c}(x_j, Q^2)], \quad (4.5)$$

with $y_i = \frac{m_{H_i}^2}{M_{W_H}^2}$, $x_j = \frac{m_{\nu_j^c}^2}{M_\Phi^2}$, $a = \frac{M_{W_H}^2}{M_{A_H}^2} = \frac{5c_W^2}{s_W^2} \sim 15$ and we have used $M_W^2/M_{W_H}^2 = v^2/(4f^2)$. Each function can be found in Appendix A. Here $V_{H\ell}^i$ are the matrix elements of the 3×3 unitary mixing matrix parametrizing the misalignment between the SM left-handed charged leptons ℓ with the heavy mirror ones ℓ_H . The W_{jk} are the matrix elements of the 3×3 unitary mixing matrix parametrizing the relative orientation of the mirror leptons and their partners ℓ^c in the $SO(5)$ (right-handed) multiplets [50].

F_L^γ can be expressed as follows [41, 50]

$$F_L^\gamma|_{Z_H} = \frac{\alpha_W}{4\pi} \frac{Q^2}{M_{W_H}^2} \sum_i V_{H\ell}^{i\mu\dagger} V_{H\ell}^{i\tau} \left(G_Z^{(1)}(y_i) + \frac{1}{5} G_Z^{(1)}(ay_i) + G_W^{(1)}(y_i) \right) \\ + \frac{\alpha_W}{4\pi} \frac{Q^2}{2M_h^2} \frac{v^4}{4f^4} \sum_{ijk} V_{H\ell}^{i\mu\dagger} \frac{m_{\ell_{Hi}}}{M_W} W_{ij}^\dagger W_{jk} \frac{m_{\ell_{Hk}}}{M_W} V_{H\ell}^{k\tau} \left(G_{\bar{\nu}^c}^{(1)}(x_j) + G_{\bar{\ell}^c}^{(1)}(x_j) \right), \quad (4.6)$$

where $G_Z^{(1)}(y)$, $G_W^{(1)}(y)$, $G_{\bar{\nu}^c}^{(1)}(x)$ and $G_{\bar{\ell}^c}^{(1)}(x)$ are defined in Appendix A.

The penguin-like diagrams with Z are given in Figure 1. Their amplitude can be expressed

$$\mathcal{M}_Z^{\text{T-odd}} = \frac{e^2}{M_Z^2} \bar{\mu}(p') [\gamma^\mu (F_L^Z P_L + F_R^Z P_R)] \tau(p) \bar{q}(p_q) [\gamma_\mu (Z_L P_L + Z_R P_R)] q(p_{\bar{q}}), \quad (4.7)$$

where

$$Z_L = \frac{g}{c_W} (T_3^q - s_W^2 Q_q), \\ Z_R = -\frac{g}{c_W} s_W^2 Q_q, \quad (4.8)$$

being

$$T_3^q = \frac{1}{2} \begin{pmatrix} 1 & & \\ & -1 & \\ & & -1 \end{pmatrix}. \quad (4.9)$$

The corresponding right-handed vector form factor F_R^Z is $\mathcal{O}(m_\tau^2/f^2)$ in the LHT and thus negligible as $f \sim \mathcal{O}(\text{TeV})$. The left-handed form factor F_L^Z , at order $\mathcal{O}(Q^2)$ according to

[50], is given by

$$\begin{aligned}
F_L^Z &= F_L^Z|_{W_H} + F_L^Z|_{A_H} + F_L^Z|_{Z_H} + F_L^Z|_{\bar{\nu}^c} + F_L^Z|_{\bar{\ell}^c} \\
&= \frac{\alpha_W}{8\pi c_W s_W} \sum_i V_{H\ell}^{i\mu\dagger} V_{H\ell}^{i\tau} \left\{ \frac{v^2}{8f^2} H_L^{W(0)}(y_i) \right. \\
&\quad \left. + \frac{Q^2}{M_{W_H}^2} \left[H_L^W(y_i) + (1 - 2c_W^2) \left(\frac{1}{5} H_L^{A/Z}(ay_i) + H_L^{A/Z}(y_i) \right) \right] \right\} \\
&\quad + \frac{\alpha_W}{8\pi c_W s_W} \frac{Q^2}{M_h^2} \frac{v^2}{2f^2} \sum_{ijk} V_{H\ell}^{i\mu\dagger} \frac{m_{\ell_{Hi}}}{M_{W_H}} W_{ij}^\dagger W_{jk} \frac{m_{\ell_{Hk}}}{M_{W_H}} V_{H\ell}^{k\tau} \left[H_L^{\bar{\nu}}(x_j) + (1 - 2c_W^2) H_L^{\bar{\ell}}(x_j) \right],
\end{aligned} \tag{4.10}$$

where all the functions definitions can be found in Appendix A.

Only the box diagram which involves interaction between $\Phi^+ \bar{\nu}_i^c \ell_j$ with $\Phi^+ \bar{u}_i^c d_j$ (and its h.c.) contributes. We show in Figure 2 all box diagrams that appear when T-odd and partner fermions are considered.

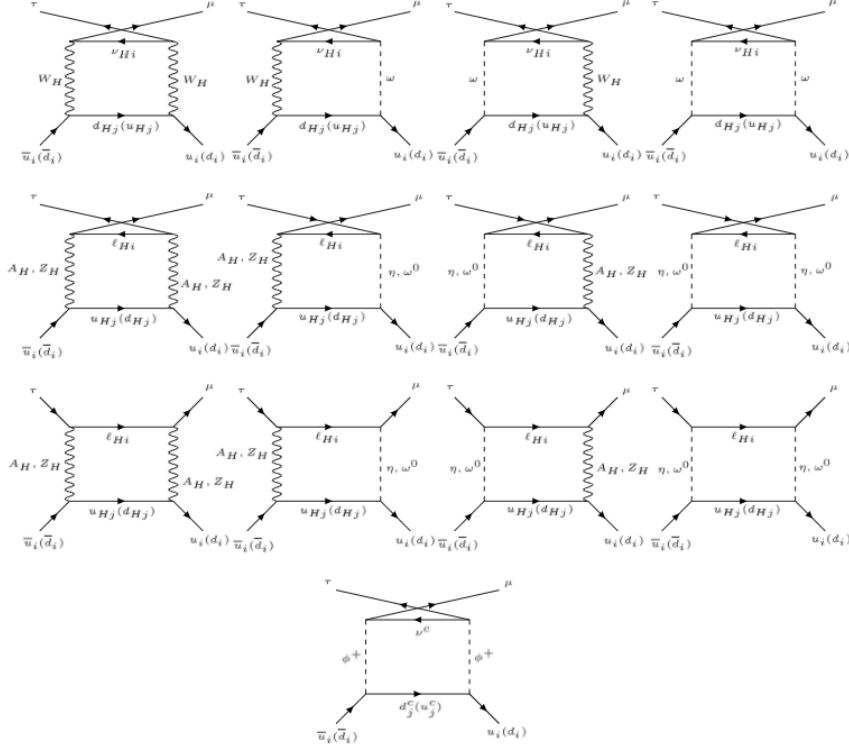


Figure 2. Box diagrams where T-odd particles, partner leptons and quarks, are involved.

The box amplitude is defined as

$$\mathcal{M}_{\text{box}}^{\text{T-odd}} = e^2 B_L^q(0) \bar{\mu}(p') \gamma^\mu P_L \tau(p) \bar{q}(p_q) \gamma_\mu P_L q(p_{\bar{q}}), \tag{4.11}$$

where $q = \{u, d, s\}$.

Therefore, in accordance to ref. [50], the form factors from box diagrams are given by

$$\begin{aligned}
B_L^u &= \frac{\alpha_W}{32\pi s_W^2} \left\{ \frac{1}{M_W^2} \frac{v^2}{4f^2} \sum_{i,j} \chi_{ij}^u \left[- \left(8 + \frac{1}{2} x_i^{\ell_H} y_j^{d_H} \right) \bar{d}_0(x_i^{\ell_H}, y_j^{d_H}) + 4x_i^{\ell_H} y_j^{d_H} d_0(x_i^{\ell_H}, y_j^{d_H}) \right. \right. \\
&\quad \left. \left. - \frac{3}{2} \bar{d}_0(x_i^{\nu_H}, y_j^{d_H}) - \frac{3}{50a} \bar{d}_0(ax_i^{\nu_H}, ay_j^{d_H}) + \frac{3}{5} \bar{d}_0(ax_i^{\nu_H}, ay_j^{d_H}, a) \right] + \frac{1}{f^2} \sum_{i,j} \bar{\chi}_{ij}^u \bar{d}_0 \left(\frac{2m_{\nu_i^c}^2}{f^2}, \frac{2m_{d_j^c}^2}{f^2} \right) \right\}, \\
B_L^d &= \frac{\alpha_W}{32\pi s_W^2} \left\{ \frac{1}{M_W^2} \frac{v^2}{4f^2} \sum_{i,j} \chi_{ij}^d \left[\left(2 + \frac{1}{2} x_i^{\ell_H} y_j^{u_H} \right) \bar{d}_0(x_i^{\ell_H}, y_j^{u_H}) - 4x_i^{\ell_H} y_j^{u_H} d_0(x_i^{\ell_H}, y_j^{u_H}) \right. \right. \\
&\quad \left. \left. - \frac{3}{2} \bar{d}_0(x_i^{\nu_H}, y_j^{u_H}) - \frac{3}{50a} \bar{d}_0(ax_i^{\nu_H}, ay_j^{u_H}) - \frac{3}{5} \bar{d}_0(ax_i^{\nu_H}, ay_j^{u_H}, a) \right] + \frac{5}{f^2} \sum_{i,j} \bar{\chi}_{ij}^d \bar{d}_0 \left(\frac{2m_{\nu_i^c}^2}{f^2}, \frac{2m_{u_j^c}^2}{f^2} \right) \right\},
\end{aligned} \tag{4.12}$$

with $x_i^{(\nu,\ell)H} = m_{(\nu,\ell)_H}^2/M_{W_H}^2$, $y_j^{(u,d)H} = (m_{H_j}^{u,d})^2/M_{W_H}^2$, $a = M_{W_H}^2/M_{A_H}^2 = 5c_W^2/s_W^2$ and the four-point functions are expressed in Appendix A.

The mixing coefficients involve mirror lepton mixing matrices as well as mirror quark ones

$$\chi_{ij}^u = V_{H\ell}^{i\mu\dagger} V_{H\ell}^{i\tau} V_{Hq}^{ju\dagger} V_{Hq}^{ju}, \quad \chi_{ij}^d = V_{H\ell}^{i\mu\dagger} V_{H\ell}^{i\tau} V_{Hq}^{jd\dagger} V_{Hq}^{jd}, \tag{4.13}$$

and

$$\begin{aligned}
\bar{\chi}_{ij}^u &= \sum_{k,n,r,s} V_{H\ell}^{k\mu\dagger} \frac{m_{\ell_{Hk}}}{M_{W_H}} W_{ki}^\dagger W_{in} \frac{m_{\ell_{Hn}}}{M_{W_H}} V_{H\ell}^{n\tau} V_{Hq}^{ru\dagger} \frac{m_{d_{Hr}}}{M_{W_H}} W_{rj}^{q\dagger} W_{js}^q \frac{m_{d_{Hs}}}{M_{W_H}} V_{Hq}^{su}, \\
\bar{\chi}_{ij}^d &= \sum_{k,n,r,s} V_{H\ell}^{k\mu\dagger} \frac{m_{\ell_{Hk}}}{M_{W_H}} W_{ki}^\dagger W_{in} \frac{m_{\ell_{Hn}}}{M_{W_H}} V_{H\ell}^{n\tau} V_{Hq}^{rd\dagger} \frac{m_{u_{Hr}}}{M_{W_H}} W_{rj}^{q\dagger} W_{js}^q \frac{m_{u_{Hs}}}{M_{W_H}} V_{Hq}^{sd}.
\end{aligned} \tag{4.14}$$

In analogy to the lepton sector, the misalignment between the partner and the mirror quarks mass eigenstates, as well as those between the mirror and SM quarks are parametrized by the corresponding 3×3 unitary matrices, V_{Hq}^i and W_{ij}^q , respectively.

4.1.2 Majorana contribution

Now, we are going to compute the \mathcal{M}^{Maj} contribution. As we showed in eq.(4.2), it is composed by three parts

$$\mathcal{M}^{\text{Maj}} = \mathcal{M}_\gamma^{\text{Maj}} + \mathcal{M}_Z^{\text{Maj}} + \mathcal{M}_{\text{box}}^{\text{Maj}}, \tag{4.15}$$

γ and Z penguin diagrams and box diagrams which involve Majorana neutrinos. In this case we will work with the assumption that light Majorana neutrinos are massless, therefore just heavy Majorana neutrinos are taken into account.

The contributions from γ - and Z -penguin diagrams and box diagrams are very similar to the ones for $\mu \rightarrow e$ conversion in nuclei:

$$\begin{aligned}\mathcal{M}_\gamma^{\text{Maj}} &= \frac{e^2}{Q^2} \bar{\mu}(p') [i2F_M^\gamma(Q^2) P_R \sigma^{\mu\nu} Q_\nu + F_L^\gamma(Q^2) \gamma^\mu P_L] \tau(p) \bar{q}(p_q) \gamma_\mu Q_q q(p_{\bar{q}}), \\ \mathcal{M}_Z^{\text{Maj}} &= \frac{e^2}{M_Z^2} \bar{\mu}(p') [\gamma^\mu (F_L^Z P_L + F_R^Z P_R)] \tau(p) \bar{q}(p_q) [\gamma_\mu (g_{Lq}^Z P_L + g_{Rq}^Z P_R)] q(p_{\bar{q}}), \\ \mathcal{M}_{\text{box}}^{\text{Maj}} &= e^2 B_L^q(0) \bar{\mu}(p') \gamma^\mu P_L \tau(p) \bar{q}(p_q) \gamma_\mu P_L q(p_{\bar{q}}),\end{aligned}\tag{4.16}$$

with Q_q , the electric charge matrix, given by

$$Q_q = \frac{1}{3} \begin{pmatrix} 2 & & \\ & -1 & \\ & & -1 \end{pmatrix},\tag{4.17}$$

in units of $|e|$ and the couplings $g_{L(R)q}^Z$ read [64]

$$\begin{aligned}g_{Lu}^Z &= \frac{1 - \frac{4}{3}s_W^2}{2s_W c_W}, & g_{Ru}^Z &= -\frac{2s_W}{3c_W}, \\ g_{Ld}^Z &= \frac{-1 + \frac{2}{3}s_W^2}{2s_W c_W}, & g_{Rd}^Z &= \frac{s_W}{3c_W}.\end{aligned}\tag{4.18}$$

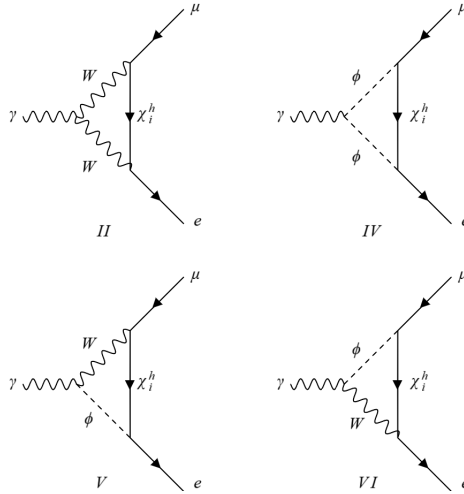


Figure 3. Feynman diagrams involved in the $\mu \rightarrow e\gamma$ decay considering heavy neutrinos. We have to take into account the self-energy diagrams, additionally. ϕ are the would-be Goldstones absorbed by W boson in the unitary gauge.

The form factors F_M^γ (from Feynman diagrams II, IV, V and VI in Figure 1), F_L^γ (from diagrams in Figure 3) and F_L^Z (see Figure 4) are given by (omitting the light Majorana

neutrinos contribution):

$$\begin{aligned}
F_M^\gamma &= F_M^{\chi^h} = \frac{\alpha_W}{16\pi} \frac{m_\tau}{M_W^2} \sum_{j=1}^3 \theta_{\mu j} \theta_{\tau j}^\dagger F_M^{\chi^h}(y_j, Q^2), \\
F_L^\gamma &= F_L^{\chi^h} = \frac{\alpha_W}{8\pi} \sum_i \theta_{\mu j} \theta_{\tau j}^\dagger F_L^{\chi^h}(y_j, Q^2), \\
F_L^{Z-\chi^h}(Q^2) &= \frac{\alpha_W}{8\pi c_W s_W} \sum_{i,j=1}^3 \left[\theta_{\mu i} \theta_{\tau i}^\dagger F^h(y_i; Q^2) + \theta_{\mu j} S_{ji} \theta_{\tau i}^\dagger \left(G^h(y_i, y_j; Q^2) + \frac{1}{\sqrt{y_i y_j}} H^h(y_i, y_j; Q^2) \right) \right].
\end{aligned} \tag{4.19}$$

The functions which define the eq. (4.19) are expressed explicitly in Appendix B.

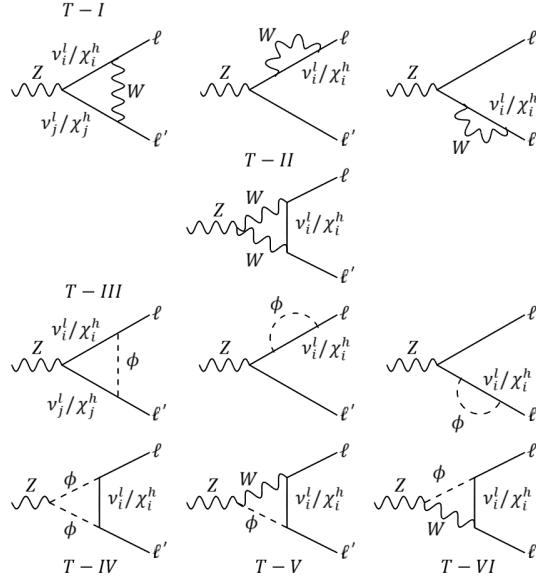


Figure 4. Z penguins diagrams that contribute to the decay. Diagrams $T - I$ and $T - III$ allow to mix light (ν_i^l) and heavy Majorana neutrinos (χ_i^h).

For box diagrams we just consider the contribution coming from heavy Majorana neutrinos χ^h in Figure 5, they read

$$B_L^d = \frac{\alpha_W}{16\pi M_W^2 s_W^2} \sum_{i,j=1}^3 \theta_{\mu i} \theta_{\tau i}^\dagger |V_{jd}|^2 f_{B_d}(y_i, x_j^u), \tag{4.20}$$

$$B_L^u = \frac{\alpha_W}{16\pi M_W^2 s_W^2} \sum_{i,j=1}^3 \theta_{\mu i} \theta_{\tau i}^\dagger |V_{uj}|^2 f_{B_u}(y_i, x_j^d), \tag{4.21}$$

where $y_i = M_W^2/M_i^2$ with M_i the mass of heavy neutrinos, $x_i^q = m_{q_i}^2/M_W^2$ with m_{q_i} the mass of the i -th quark, V_{ij} is the CKM matrix. Neglecting all quark masses, except that of the top quark, and defining $x_t = m_t^2/M_W^2$, we may write [64]:

$$\sum_{i=j}^3 |V_{jd}|^2 f_{B_d}(y_i, x_j^u) = |V_{td}|^2 [f_{B_d}(y_i, x_t) - f_{B_d}(y_i, 0)] - f_{B_d}(y_i, 0), \tag{4.22}$$

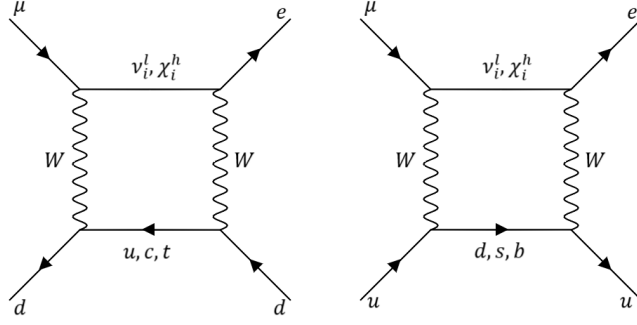


Figure 5. Box diagrams contributing to $\mu-e$ conversion in nuclei considering light-heavy Majorana neutrinos.

$$\sum_{i=j}^3 |V_{uj}|^2 f_{Bu}(y_i, x_j^d) = f_{Bu}(y_i, 0), \quad (4.23)$$

with $x_t = m_t^2/M_W^2$.

4.2 Hadronization

Tau decays we are considering have as final states pseudoscalar mesons and vector resonances. Hadronization of quark bilinears gives rise to the final-state hadrons.

Resonance Chiral Theory (R χ T) [65, 66], that naturally includes Chiral Perturbation Theory (χ PT) [67, 68], considers the resonances as active degrees of freedom into the Lagrangian since they drive the dynamics of the processes. We are working under R χ T scheme in order to hadronize the relevant currents involved in our analysis. For more details on the procedure followed in this part, see refs. [62, 69] where the definitions of all expressions are fully given. In Appendix C we write all the useful tools for the development which is shown next.

We remind that the complete amplitude has two contributions:

$$\mathcal{M} = \mathcal{M}^{\text{T-odd}} + \mathcal{M}^{\text{Maj}}, \quad (4.24)$$

where each one receives contributions coming from γ - and Z -penguins, and box diagrams. The F_M^γ form factor, considering both contributions of T-odd leptons (eq. (4.5)) and Majorana neutrinos (eq. (4.19)), is written as follows

$$\begin{aligned} F_M^\gamma = & \frac{\alpha_W}{16\pi} \frac{m_\tau}{M_W^2} \left\{ \sum_{i=1}^3 \left(\theta_{\mu i} \theta_{\tau i}^\dagger F_M^{\chi^h}(z_i, Q^2) \right. \right. \\ & + \frac{v^2}{4f^2} V_{H\ell}^{i\mu*} V_{H\ell}^{i\tau} \left[F_{W_H}(x_i^{\ell H}, Q^2) + F_{Z_H}(x_i^{\nu H}, Q^2) + \frac{1}{5} F_{Z_H}(ax_i^{\nu H}, Q^2) \right] \Big) \\ & \left. + \frac{1}{M_h^2} \frac{v^4}{4f^2} \sum_{i,j,k=1}^3 V_{H\ell}^{i\mu\dagger} \kappa_{ii} W_{ij}^\dagger W_{jk} \kappa_{kk} V_{H\ell}^{k\tau} \left[F_{\bar{\nu}^c} \left(\frac{2m_{\nu_j^c}^2}{f^2}, Q^2 \right) + F_{\bar{\ell}^c} \left(\frac{2m_{\ell_j^c}^2}{f^2}, Q^2 \right) \right] \right\}, \end{aligned} \quad (4.25)$$

where $z_i = M_W^2/M_i^2$, with M_i the heavy Majorana neutrino masses, and we recall that $x_i^{(\nu,\ell)H} = m_{(\nu,\ell)H}^2/M_{WH}^2$, $y_j^{(u,d)H} = (m_{Hj}^{u,d})^2/M_{WH}^2$, $a = M_{WH}^2/M_{AH}^2 = 5c_W^2/s_W^2$.

Similarly, F_L^γ can be written from eqs. (4.6) and (4.19) as

$$F_L^\gamma = \frac{\alpha_W}{4\pi M_W^2} \left\{ \sum_{i=1}^3 \left(\frac{1}{2} \theta_{\mu i} \theta_{\tau i}^\dagger F_L^{\chi^h}(z_i, Q^2) \right. \right. \\ \left. \left. + M_W^2 \frac{Q^2}{M_{WH}^2} V_{H\ell}^{i\mu*} V_{H\ell}^{i\tau} \left[G_W^{(1)}(x_i^{\ell_H}) + G_Z^{(1)}(x_i^{\nu_H}) + \frac{1}{5} G_Z^{(1)}(ax_i^{\nu_H}) \right] \right) \right. \\ \left. + v^2 \frac{M_W^2}{M_h^2} \frac{Q^2}{M_{WH}^2} \sum_{i,j,k=1}^3 V_{H\ell}^{i\mu\dagger} \kappa_{ii} W_{ij}^\dagger W_{jk} \kappa_{kk} V_{H\ell}^{k\tau} \left[G_{\bar{\nu}^c}^{(1)} \left(\frac{2m_{\nu_i^c}^2}{f^2} \right) + G_{\bar{\ell}^c}^{(1)} \left(\frac{2m_{\nu_j^c}^2}{f^2} \right) \right] \right\}. \quad (4.26)$$

The form factor coming from Z -penguin diagrams, taking into account T-odd particles (eq. (4.10)) as well as Majorana neutrinos (eq. (4.19)) reads

$$F_L^Z = \frac{\alpha_W}{8\pi c_W s_W} \sum_{i,j=1}^3 \left[\theta_{\mu i} \theta_{\tau i}^\dagger F^h(z_i; Q^2) + \theta_{\mu j} S_{ji} \theta_{\tau i}^\dagger \left(G^h(z_i, z_j; Q^2) + \frac{1}{\sqrt{z_i, z_j}} H^h(z_i, z_j; Q^2) \right) \right. \\ \left. + \sum_i V_{H\ell}^{i\mu\dagger} V_{H\ell}^{i\tau} \left\{ \frac{v^2}{8f^2} H_L^{W(0)}(x_i^{\ell_H}) + \frac{Q^2}{M_{WH}^2} \left[H_L^W(x_i^{\ell_H}) + (1 - 2c_W^2) \left(\frac{1}{5} H_L^{A/Z}(ax_i^{\nu_H}) + H_L^{A/Z}(x_i^{\nu_H}) \right) \right] \right\} \right. \\ \left. + \frac{Q^2}{M_\Phi^2} \frac{v^2}{2M_W^2} \sum_{ijk} V_{H\ell}^{i\mu\dagger} \kappa_{ii} W_{ij}^\dagger W_{jk} \kappa_{kk} V_{H\ell}^{k\tau} \left[H_L^{\bar{\nu}} \left(\frac{2m_{\nu_j^c}^2}{f^2} \right) + (1 - 2c_W^2) H_L^{\bar{\ell}} \left(\frac{2m_{\nu_j^c}^2}{f^2} \right) \right] \right]. \quad (4.27)$$

For box diagrams the B_L^q form factors are given by eqs. (4.12), (4.20) and (4.21), yielding

$$B_L^u = \frac{\alpha_W}{16\pi M_W^2 s_W^2} \left\{ \sum_{i,j=1}^3 \theta_{\mu i} \theta_{\tau i}^\dagger f_{B_u}(z_i, 0) \right. \\ \left. - \frac{v^2}{8f^2} \sum_{i,j} \chi_{ij}^u \left[\left(8 + \frac{1}{2} x_i^{\ell_H} y_j^{dH} \right) \bar{d}_0(x_i^{\ell_H}, y_j^{dH}) - 4x_i^{\ell_H} y_j^{dH} d_0(x_i^{\ell_H}, y_j^{dH}) \right. \right. \\ \left. \left. + \frac{3}{2} \bar{d}_0(x_i^{\nu_H}, y_j^{dH}) + \frac{3}{50a} \bar{d}_0(ax_i^{\nu_H}, ay_j^{dH}) - \frac{3}{5} \bar{d}_0(ax_i^{\nu_H}, ay_j^{dH}, a) \right] + \frac{M_W^2}{2f^2} \sum_{i,j} \bar{\chi}_{ij}^u \bar{d}_0 \left(\frac{2m_{\nu_i^c}^2}{f^2}, \frac{2m_{d_j^c}^2}{f^2} \right) \right\}, \quad (4.28)$$

$$B_L^d = \frac{\alpha_W}{16\pi M_W^2 s_W^2} \left\{ \sum_{i,j=1}^3 \theta_{\mu i} \theta_{\tau i}^\dagger (|V_{td}|^2 [f_{B_d}(z_i, x_t) - f_{B_d}(z_i, 0)] - f_{B_d}(z_i, 0)) \right. \\ \left. + \frac{v^2}{8f^2} \sum_{i,j} \chi_{ij}^d \left[\left(2 + \frac{1}{2} x_i^{\ell_H} y_j^{uH} \right) \bar{d}_0(x_i^{\ell_H}, y_j^{uH}) - 4x_i^{\ell_H} y_j^{uH} d_0(x_i^{\ell_H}, y_j^{uH}) \right. \right. \\ \left. \left. - \frac{3}{2} \bar{d}_0(x_i^{\nu_H}, y_j^{uH}) - \frac{3}{50a} \bar{d}_0(ax_i^{\nu_H}, ay_j^{uH}) - \frac{3}{5} \bar{d}_0(ax_i^{\nu_H}, ay_j^{uH}, a) \right] + \frac{5}{2} \frac{M_W^2}{f^2} \sum_{i,j} \bar{\chi}_{ij}^d \bar{d}_0 \left(\frac{2m_{\nu_i^c}^2}{f^2}, \frac{2m_{u_j^c}^2}{f^2} \right) \right\}. \quad (4.29)$$

4.3 $\tau \rightarrow \ell P$ ($\ell = e, \mu$)

These decays, where $P = \{\pi^0, \eta, \eta'\}$, are mediated only by axial-vector current (Z gauge boson) and box diagrams. Thus, the amplitude is given by

$$\mathcal{M}_{\tau \rightarrow \mu P} = \mathcal{M}_Z^P + \mathcal{M}_{\text{Box}}^P. \quad (4.30)$$

From Appendix C each contribution reads

$$\begin{aligned} \mathcal{M}_Z^P &= -i \frac{g^2}{2c_W} \frac{F}{M_Z^2} C(P) \sum_i \bar{\mu}(p') [\mathcal{Q} F_L^Z P_L] \tau(p), \\ \mathcal{M}_{\text{Box}}^P &= -ig^2 F \sum_i B_i(P) \bar{\mu}(p') [\mathcal{Q} P_L] \tau(p), \end{aligned} \quad (4.31)$$

where $C(P)$ and $B_j(P)$ functions are shown in Appendix C, $F \simeq 0.0922$ GeV is the pion decay constant, F_L^Z is given by eq. (4.27) and, as we know, F_R^Z is negligible.

Then we can write explicitly the amplitude for each decay considering $P = \{\pi^0, \eta, \eta'\}$. Mixing effects among these particles, which are isospin-suppressed (see e.g. [70]), are negligible.

4.3.1 $\tau \rightarrow \mu \pi^0$

In this case where we are considering that $P = \pi^0$, with $\pi^0 = \frac{u\bar{u} - d\bar{d}}{\sqrt{2}}$, taking into account the $C(P)$ and $B_j(P)$ functions from Appendix C, the contributions to the amplitude become

$$\begin{aligned} \mathcal{M}_Z^{\pi^0} &= -i \frac{g^2}{2c_W} \frac{F}{M_Z^2} C(\pi^0) \bar{\mu}(p') [\mathcal{Q} F_L^Z P_L] \tau(p) = -i \frac{g^2}{2c_W} \frac{F}{M_Z^2} \bar{\mu}(p') [\mathcal{Q} F_L^Z P_L] \tau(p), \\ \mathcal{M}_{\text{Box}}^{\pi^0} &= -ig^2 F B(\pi^0) \bar{\mu}(p') [\mathcal{Q} P_L] \tau(p) = -ig^2 F \frac{1}{2} (B_L^d - B_L^u) \bar{\mu}(p') [\mathcal{Q} P_L] \tau(p). \end{aligned} \quad (4.32)$$

Unlike the expressions from Appendix C, in the equation above the sum over the mixing matrices does not appear because it is included within the form factors F_L^Z and B_L^q , which are defined in eqs. (4.27), (4.28) and (4.29).

We can write the branching ratio of this decay as follows

$$\text{Br}(\tau \rightarrow \mu \pi^0) = \frac{1}{4\pi} \frac{\lambda^{1/2}(m_\tau^2, m_\mu^2, m_{\pi^0}^2)}{m_\tau^2 \Gamma_\tau} \frac{1}{2} \sum_{i,f} |\mathcal{M}_{\tau \rightarrow \mu \pi^0}|^2, \quad (4.33)$$

where $\mathcal{M}_{\tau \rightarrow \mu P}$ is defined in eq. (C.6). Hence, it yields

$$\sum_{i,f} |\mathcal{M}_{\tau \rightarrow \mu \pi^0}|^2 = \frac{1}{2m_\tau} \sum_{k,l} \left[(m_\tau^2 + m_\mu^2 - m_{\pi^0}^2) (a_{\pi^0}^k a_{\pi^0}^{l*} + b_{\pi^0}^k b_{\pi^0}^{l*}) + 2m_\mu m_\tau (a_{\pi^0}^k a_{\pi^0}^{l*} - b_{\pi^0}^k b_{\pi^0}^{l*}) \right]. \quad (4.34)$$

Considering from [11] $m_{\pi^0} = 134.9768$ MeV, $m_\mu = 105.6583$ MeV, and $m_\tau = 1776.86$ MeV,

$$\begin{aligned} \sum_{i,f} |\mathcal{M}_{\tau \rightarrow \mu \pi^0}|^2 &= \frac{1}{2m_\tau} \sum_{k,l} \left[(m_\tau^2 + m_\mu^2 - m_{\pi^0}^2) (a_{\pi^0}^k a_{\pi^0}^{l*} + b_{\pi^0}^k b_{\pi^0}^{l*}) + 2m_\mu m_\tau (a_{\pi^0}^k a_{\pi^0}^{l*} - b_{\pi^0}^k b_{\pi^0}^{l*}) \right], \\ &\approx (886.44 \text{ MeV}) \sum_{k,l} \left[1.12 a_{\pi^0}^k a_{\pi^0}^{l*} + 0.88 b_{\pi^0}^k b_{\pi^0}^{l*} \right]. \end{aligned} \quad (4.35)$$

Numerical coefficients in the previous equation and the corresponding ones for $P = \eta, \eta'$ are important for understanding correlations between these channels later on.

The generic expressions for a_P^k and b_P^k are indicated in eq. (C.13), for $P = \pi^0$ they become

$$\begin{aligned} a_{\pi^0}^Z &= -\frac{1}{2M_Z^2 s_W^2 c_W} \frac{F}{2} \Delta_{\tau\mu} F_L^Z, \\ b_{\pi^0}^Z &= -\frac{1}{2M_Z^2 s_W^2 c_W} \frac{F}{2} \Sigma_{\tau\mu} F_L^Z, \\ a_{\pi^0}^B &= -\frac{F}{2s_W^2} \Delta_{\tau\mu} \frac{1}{2} (B_L^d - B_L^u), \\ b_{\pi^0}^B &= -\frac{F}{2s_W^2} \Sigma_{\tau\mu} \frac{1}{2} (B_L^d - B_L^u). \end{aligned} \quad (4.36)$$

4.3.2 $\tau \rightarrow \mu\eta$

Considering $P = \eta$ with $\eta \approx \frac{1}{\sqrt{6}}(u\bar{u} + d\bar{d} - 2s\bar{s})$ ⁴, and $C(P)$ and $B_j(P)$ functions from Appendix C, the contributions to the amplitude are given by ($\theta_\eta \simeq -18^\circ$)

$$\begin{aligned} \mathcal{M}_Z^\eta &= -i \frac{g^2}{2c_W} \frac{F}{M_Z^2} \frac{1}{\sqrt{6}} \left(\sin \theta_\eta + \sqrt{2} \cos \theta_\eta \right) \bar{\mu}(p') [\not{Q} F_L^Z P_L] \tau(p), \\ \mathcal{M}_{\text{Box}}^\eta &= -ig^2 F \frac{1}{2\sqrt{3}} \left[(\sqrt{2} \sin \theta_\eta - \cos \theta_\eta) B_L^u + (2\sqrt{2} \sin \theta_\eta + \cos \theta_\eta) B_L^d \right] \bar{\mu}(p') [\not{Q} P_L] \tau(p). \end{aligned} \quad (4.37)$$

The branching ratio then reads

$$\text{Br}(\tau \rightarrow \mu\eta) = \frac{1}{4\pi} \frac{\lambda^{1/2}(m_\tau^2, m_\mu^2, m_\eta^2)}{m_\tau^2 \Gamma_\tau} \frac{1}{2} \sum_{i,f} |\mathcal{M}_{\tau \rightarrow \mu\eta}|^2, \quad (4.38)$$

where $\mathcal{M}_{\tau \rightarrow \mu\eta}$ yields

$$\sum_{i,f} |\mathcal{M}_{\tau \rightarrow \mu\eta}|^2 = \frac{1}{2m_\tau} \sum_{k,l} \left[(m_\tau^2 + m_\mu^2 - m_\eta^2) (a_\eta^k a_\eta^{l*} + b_\eta^k b_\eta^{l*}) + 2m_\mu m_\tau (a_\eta^k a_\eta^{l*} - b_\eta^k b_\eta^{l*}) \right]. \quad (4.39)$$

From [11] $m_\eta = 547.862$ MeV and $m_{\mu,\tau}$ given previously, we get

$$\begin{aligned} \sum_{i,f} |\mathcal{M}_{\tau \rightarrow \mu\eta}|^2 &= \frac{1}{2m_\tau} \sum_{k,l} \left[(m_\tau^2 + m_\mu^2 - m_\eta^2) (a_\eta^k a_\eta^{l*} + b_\eta^k b_\eta^{l*}) + 2m_\mu m_\tau (a_\eta^k a_\eta^{l*} - b_\eta^k b_\eta^{l*}) \right], \\ &\approx (807.10 \text{ MeV}) \sum_{k,l} \left[1.13 a_\eta^k a_\eta^{l*} + 0.87 b_\eta^k b_\eta^{l*} \right]. \end{aligned} \quad (4.40)$$

⁴A more refined hadronization requires using the double-angle mixing scheme for the $\eta - \eta'$ mesons [71]. See, for instance, Refs. [72, 73].

For $P = \eta$ from eqs. (C.9) and (C.10) the a_P^k and b_P^k factors turn out to be

$$\begin{aligned} a_\eta^Z &= -\frac{g^2}{2M_Z^2 c_W} \frac{F}{2} \frac{1}{\sqrt{6}} \left(\sin \theta_\eta + \sqrt{2} \cos \theta_\eta \right) \Delta_{\tau\mu} F_L^Z, \\ b_\eta^Z &= -\frac{g^2}{2M_Z^2 c_W} \frac{F}{2} \frac{1}{\sqrt{6}} \left(\sin \theta_\eta + \sqrt{2} \cos \theta_\eta \right) \Sigma_{\tau\mu} F_L^Z, \\ a_\eta^B &= -\frac{g^2 F}{2} \Delta_{\tau\mu} \frac{1}{2\sqrt{3}} \left[(\sqrt{2} \sin \theta_\eta - \cos \theta_\eta) B_L^u + (2\sqrt{2} \sin \theta_\eta + \cos \theta_\eta) B_L^d \right], \\ b_\eta^B &= -\frac{g^2 F}{2} \Sigma_{\tau\mu} \frac{1}{2\sqrt{3}} \left[(\sqrt{2} \sin \theta_\eta - \cos \theta_\eta) B_L^u + (2\sqrt{2} \sin \theta_\eta + \cos \theta_\eta) B_L^d \right]. \end{aligned} \quad (4.41)$$

4.3.3 $\tau \rightarrow \mu\eta'$

For the $P = \eta'$ case, with $\eta' \approx \frac{1}{\sqrt{3}}(u\bar{u} + d\bar{d} + s\bar{s})$, taking the $C(P)$ and $B_j(P)$ functions from Appendix C, the amplitude contributions are written as follows

$$\begin{aligned} \mathcal{M}_Z^\eta &= -i \frac{g^2}{2c_W} \frac{F}{M_Z^2} \frac{1}{\sqrt{6}} \left(\sqrt{2} \sin \theta_\eta - \cos \theta_\eta \right) \bar{\mu}(p') [\not{Q} F_L^Z P_L] \tau(p), \\ \mathcal{M}_{\text{Box}}^\eta &= -ig^2 F \frac{1}{2\sqrt{3}} \left[(\sin \theta_\eta - 2\sqrt{2} \cos \theta_\eta) B_L^d - (\sin \theta_\eta + \sqrt{2} \cos \theta_\eta) B_L^u \right] \bar{\mu}(p') [\not{Q} P_L] \tau(p). \end{aligned} \quad (4.42)$$

The branching fraction is given by

$$\text{Br}(\tau \rightarrow \mu\eta') = \frac{1}{4\pi} \frac{\lambda^{1/2}(m_\tau^2, m_\mu^2, m_{\eta'}^2)}{m_\tau^2 \Gamma_\tau} \frac{1}{2} \sum_{i,f} |\mathcal{M}_{\tau \rightarrow \mu\eta'}|^2, \quad (4.43)$$

where $\mathcal{M}_{\tau \rightarrow \mu\eta'}$ yields

$$\sum_{i,f} |\mathcal{M}_{\tau \rightarrow \mu\eta'}|^2 = \frac{1}{2m_\tau} \sum_{k,l} \left[(m_\tau^2 + m_\mu^2 - m_{\eta'}^2) (a_{\eta'}^k a_{\eta'}^{l*} + b_{\eta'}^k b_{\eta'}^{l*}) + 2m_\mu m_\tau (a_{\eta'}^k a_{\eta'}^{l*} - b_{\eta'}^k b_{\eta'}^{l*}) \right]. \quad (4.44)$$

From [11] $m_{\eta'} = 957.78$ MeV and $m_{\mu,\tau}$ given previously, we obtain

$$\begin{aligned} \sum_{i,f} |\mathcal{M}_{\tau \rightarrow \mu\eta'}|^2 &= \frac{1}{2m_\tau} \sum_{k,l} \left[(m_\tau^2 + m_\mu^2 - m_{\eta'}^2) (a_{\eta'}^k a_{\eta'}^{l*} + b_{\eta'}^k b_{\eta'}^{l*}) + 2m_\mu m_\tau (a_{\eta'}^k a_{\eta'}^{l*} - b_{\eta'}^k b_{\eta'}^{l*}) \right], \\ &\approx (633.43 \text{ MeV}) \sum_{k,l} \left[1.17 a_{\eta'}^k a_{\eta'}^{l*} + 0.83 b_{\eta'}^k b_{\eta'}^{l*} \right]. \end{aligned} \quad (4.45)$$

For $P = \eta'$ from eq. (C.9) and (C.10) in Appendix C the a_P^k and b_P^k factors become

$$\begin{aligned} a_{\eta'}^Z &= -\frac{g^2}{2M_Z^2 c_W} \frac{F}{2} \frac{1}{\sqrt{6}} \left(\sqrt{2} \sin \theta_\eta - \cos \theta_\eta \right) \Delta_{\tau\mu} F_L^Z, \\ b_{\eta'}^Z &= -\frac{g^2}{2M_Z^2 c_W} \frac{F}{2} \frac{1}{\sqrt{6}} \left(\sqrt{2} \sin \theta_\eta - \cos \theta_\eta \right) \Sigma_{\tau\mu} F_L^Z, \\ a_{\eta'}^B &= -\frac{g^2 F}{2} \Delta_{\tau\mu} \frac{1}{2\sqrt{3}} \left[(\sin \theta_\eta - 2\sqrt{2} \cos \theta_\eta) B_L^d - (\sin \theta_\eta + \sqrt{2} \cos \theta_\eta) B_L^u \right], \\ b_{\eta'}^B &= -\frac{g^2 F}{2} \Sigma_{\tau\mu} \frac{1}{2\sqrt{3}} \left[(\sin \theta_\eta - 2\sqrt{2} \cos \theta_\eta) B_L^d - (\sin \theta_\eta + \sqrt{2} \cos \theta_\eta) B_L^u \right]. \end{aligned} \quad (4.46)$$

4.4 $\tau \rightarrow \ell PP$ ($\ell = e, \mu$)

In this part we will consider the decays into the pairs $P\bar{P} = \{\pi^+\pi^-, K^+K^-, K^0\bar{K}^0\}$ (others are CKM- or isospin-suppressed). The contributions to this kind of decays come from γ -, Z - penguins and box diagrams. Thus, the total amplitude can be written as follows

$$\mathcal{M}_{\tau \rightarrow \mu PP} = \mathcal{M}_{\gamma}^{P\bar{P}} + \mathcal{M}_Z^{P\bar{P}} + \mathcal{M}_{\text{Box}}^{P\bar{P}}. \quad (4.47)$$

Using the expressions shown in Appendix C we hadronize the quark bilinears and get the contributions for each decay, that are presented next.

4.4.1 $\tau \rightarrow \mu \pi^+ \pi^-$

As mentioned earlier, the total amplitude receives three contributions coming from γ -, Z - penguins and box diagrams, hence the amplitude for this decay is

$$\mathcal{M}_{\tau \rightarrow \mu \pi^+ \pi^-} = \mathcal{M}_{\gamma}^{\pi^+ \pi^-} + \mathcal{M}_Z^{\pi^+ \pi^-} + \mathcal{M}_{\text{Box}}^{\pi^+ \pi^-}, \quad (4.48)$$

where each amplitude is given by eq. (C.16) (see Appendix C) ⁵

$$\begin{aligned} \mathcal{M}_{\gamma}^{\pi^+ \pi^-} &= \frac{e^2}{Q^2} F_V^{\pi\pi}(s) \bar{\mu}(p') [Q^2 (\not{p}_q - \not{p}_{\bar{q}}) F_L^{\gamma}(Q^2) P_L + 2im_{\tau} p_q^{\mu} \sigma_{\mu\nu} p_{\bar{q}}^{\nu} F_M^{\gamma}(Q^2) P_R] \tau(p), \\ \mathcal{M}_Z^{\pi^+ \pi^-} &= g^2 \frac{2s_W^2 - 1}{2c_W M_Z^2} F_V^{\pi\pi}(s) \bar{\mu}(p') (\not{p}_q - \not{p}_{\bar{q}}) [F_L^Z P_L] \tau(p), \\ \mathcal{M}_{\text{Box}}^{\pi^+ \pi^-} &= \frac{g^2}{2} F_V^{\pi\pi}(s) (B_L^u - B_L^d) \bar{\mu}(p') (\not{p}_q - \not{p}_{\bar{q}}) P_L \tau(p), \end{aligned} \quad (4.49)$$

The vector form factor $F_V^{\pi\pi}$ is given by eq. (D.3) in Appendix D.

From Appendix C the branching ratio for this decay yields

$$\text{Br}(\tau \rightarrow \mu \pi^+ \pi^-) = \frac{1}{64\pi^3 m_{\tau}^2 \Gamma_{\tau}} \int_{s_-}^{s_+} ds \int_{t_-}^{t_+} dt \frac{1}{2} \sum_{i,f} |\mathcal{M}_{\tau \rightarrow \mu \pi^+ \pi^-}|^2, \quad (4.50)$$

where $s = (p_q + p_{\bar{q}})^2$ and $t = (p - p_{\bar{q}})^2$, so the integration limits are

$$\begin{aligned} t_{\pm}^+ &= \frac{1}{4s} \left[(m_{\tau}^2 - m_{\mu}^2)^2 - \left(\lambda^{1/2}(s, m_{\pi^+}^2, m_{\pi^-}^2) \mp \lambda^{1/2}(m_{\tau}^2, s, m_{\mu}^2) \right)^2 \right], \\ s_- &= 4m_{\pi^+}^2, \\ s_+ &= (m_{\tau} - m_{\mu})^2. \end{aligned} \quad (4.51)$$

4.4.2 $\tau \rightarrow \mu K^+ K^-$

The total amplitude for this decays reads as

$$\mathcal{M}_{\tau \rightarrow \mu K^+ K^-} = \mathcal{M}_{\gamma}^{K^+ K^-} + \mathcal{M}_Z^{K^+ K^-} + \mathcal{M}_{\text{Box}}^{K^+ K^-}, \quad (4.52)$$

⁵We recall that the sum over the mixing matrices does not appear because it is included within the form factors.

where from Appendix C each amplitude can be written

$$\begin{aligned}
\mathcal{M}_\gamma^{K^+K^-} &= \frac{e^2}{Q^2} F_V^{K^+K^-}(s) \bar{\mu}(p') [Q^2(\not{p}_q - \not{p}_{\bar{q}}) F_L^\gamma(Q^2) P_L + 2im_\tau p_q^\mu \sigma_{\mu\nu} p_{\bar{q}}^\nu F_M^\gamma(Q^2) P_R] \tau(p), \\
\mathcal{M}_Z^{K^+K^-} &= g^2 \frac{2s_W^2 - 1}{2c_W M_Z^2} F_V^{K^+K^-}(s) \bar{\mu}(p') (\not{p}_q - \not{p}_{\bar{q}}) [F_L^Z P_L] \tau(p), \\
\mathcal{M}_{\text{Box}}^{K^+K^-} &= \frac{g^2}{2} F_V^{K^+K^-}(s) (B_L^u - B_L^d) \bar{\mu}(p') (\not{p}_q - \not{p}_{\bar{q}}) P_L \tau(p),
\end{aligned} \tag{4.53}$$

the vector form factor $F_V^{K^+K^-}$ is shown in Appendix D. The branching ratio expression is analogous to $\tau \rightarrow \mu \pi^+ \pi^+$, just replacing m_π by m_K in the integral limits.

4.4.3 $\tau \rightarrow \mu K^0 \bar{K}^0$

The total amplitude is given by

$$\mathcal{M}_{\tau \rightarrow \mu K^0 \bar{K}^0} = \mathcal{M}_\gamma^{K^0 \bar{K}^0} + \mathcal{M}_Z^{K^0 \bar{K}^0} + \mathcal{M}_{\text{Box}}^{K^0 \bar{K}^0}. \tag{4.54}$$

From Appendix C each amplitude is expressed as follows

$$\begin{aligned}
\mathcal{M}_\gamma^{K^0 \bar{K}^0} &= \frac{e^2}{Q^2} F_V^{K^0 \bar{K}^0}(s) \bar{\mu}(p') [Q^2(\not{p}_q - \not{p}_{\bar{q}}) F_L^\gamma(Q^2) P_L + 2im_\tau p_q^\mu \sigma_{\mu\nu} p_{\bar{q}}^\nu F_M^\gamma(Q^2) P_R] \tau(p), \\
\mathcal{M}_Z^{K^0 \bar{K}^0} &= g^2 \frac{2s_W^2 - 1}{2c_W M_Z^2} F_V^{K^0 \bar{K}^0}(s) \bar{\mu}(p') (\not{p}_q - \not{p}_{\bar{q}}) [F_L^Z P_L] \tau(p), \\
\mathcal{M}_{\text{Box}}^{K^0 \bar{K}^0} &= \frac{g^2}{2} F_V^{K^0 \bar{K}^0}(s) (B_L^u - B_L^d) \bar{\mu}(p') (\not{p}_q - \not{p}_{\bar{q}}) P_L \tau(p),
\end{aligned} \tag{4.55}$$

with $F_V^{K^0 \bar{K}^0}$ given in Appendix D. The branching ratio can be obtained from eq. (C.17) with $m_{P_1} = m_{P_2} = m_{K^0}$ in the limits of the integral.

4.5 $\tau \rightarrow \ell V$ ($\ell = e, \mu$, $V = \rho, \phi$)

The calculation of observables involving hadron resonances as external states is not properly defined within quantum field theory because hadron resonances decay strongly and are not proper asymptotic states, as is required in that framework. When an experiment measures a final state with a vector resonance, the experiment reconstructs its structure from the pair of pseudoscalar mesons with a squared total mass approaching m_V^2 , where $V = \rho, \phi$. For instance, from the chiral point of view, two pions in a $J = I = 1$ state are indistinguishable from a ρ . Then, following the expressions from Appendix C the branching ratios can be obtained. The procedure is very similar to $\tau \rightarrow \mu PP$ decays, we need to compute the same integral (eq. C.17) where now the limits on s are different. They are given by eq. (C.20).

5 Phenomenology

First of all, we recall the masses of particles which come from LHT that are involved in the processes under study [41, 54, 74]:

$$\begin{aligned} M_W &= \frac{v}{2s_W} \left(1 - \frac{v^2}{12f^2} \right), \quad M_Z = M_W/c_W, \quad v \simeq 246 \text{ GeV}, \quad (\rho \text{ factor is conserved}), \\ M_{W_H} &= M_{Z_H} = \frac{f}{s_W} \left(1 - \frac{v^2}{8f^2} \right), \quad M_{A_H} = \frac{f}{\sqrt{5}c_W} \left(1 - \frac{5v^2}{8f^2} \right), \quad M_\Phi = \sqrt{2}M_h \frac{f}{v}, \\ m_{\ell_H^i} &= \sqrt{2}\kappa_{ii}f \equiv m_{Hi}, \quad m_{\nu_H^i} = m_{Hi} \left(1 - \frac{v^2}{8f^2} \right), \quad m_{\ell^c, \nu^c} = \kappa_2, \end{aligned} \quad (5.1)$$

with M_h being the mass of the SM Higgs scalar, κ_{ii} the diagonal entries of the κ matrix (see eq. (2.8)) (similarly for the masses of T-odd quarks with κ_{ii}^q instead of κ_{ii} and replacing d_H -quark by ℓ_H and u_H -quark by ν_H) and κ_2 the mass matrix of partner leptons from eq. (2.8) (κ_2^q similarly for partner quarks of u and d types). Due to $M_h = 125.25 \pm 0.17 \text{ GeV}$ [11] and $v \simeq 246 \text{ GeV}$, we can approximate

$$M_\Phi = \sqrt{2}M_h \frac{f}{v} \approx \frac{\sqrt{2}}{2}f. \quad (5.2)$$

So far, the free parameters are: f (scale of new physics); κ_{ii} and κ_{ii}^q (Yukawa couplings for T-odd leptons and quarks); κ_2 and κ_2^q , mass matrices for partner leptons.

The expressions χ_{ij}^u , χ_{ij}^d , $\bar{\chi}_{ij}^u$ and $\bar{\chi}_{ij}^d$ (see eq. (4.14)) describe the interaction vertices from box diagrams, those can be re-written in terms of free parameters as follows

$$\begin{aligned} \bar{\chi}_{ij}^u &= \frac{v^4}{4M_W^4} \sum_{k,n,r,s} V_{H\ell}^{k\mu\dagger} \kappa_{kk} W_{ki}^\dagger W_{in} \kappa_{nn} V_{H\ell}^{n\tau} V_{Hq}^{ru\dagger} \kappa_{rr}^d W_{rj}^{q\dagger} W_{js}^q \kappa_{ss}^d V_{Hq}^{su}, \\ \bar{\chi}_{ij}^d &= \frac{v^4}{4M_W^4} \left(1 - \frac{v^2}{8f^2} \right)^2 \sum_{k,n,r,s} V_{H\ell}^{k\mu\dagger} \kappa_{kk} W_{ki}^\dagger W_{in} \kappa_{nn} V_{H\ell}^{n\tau} V_{Hq}^{rd\dagger} \kappa_{rr}^u W_{rj}^{q\dagger} W_{js}^q \kappa_{ss}^u V_{Hq}^{sd}, \end{aligned} \quad (5.3)$$

where we see a small shift between interaction vertices of order $\mathcal{O}(v^2/8f^2)$. The mixing matrices of heavy Majorana neutrinos are bounded by [52]

$$|\theta_{ej}\theta_{\tau j}^\dagger| < 0.95 \times 10^{-2}, \quad |\theta_{\mu j}\theta_{\tau j}^\dagger| < 0.011. \quad (5.4)$$

Considering just mixing between two lepton families, the mixing matrix of T-odd leptons ($V_{H\ell}^{i\mu*} V_{H\ell}^{i\tau}$) and the mixing matrix among partner leptons ($W_{ij}^{i\mu\dagger} W_{jk}^{i\tau}$) can be parameterized as follows [50]

$$V = \begin{pmatrix} 1 & 0 & 0 \\ 0 & \cos \theta_V & \sin \theta_V \\ 0 & -\sin \theta_V & \cos \theta_V \end{pmatrix}, \quad W = \begin{pmatrix} 1 & 0 & 0 \\ 0 & \cos \theta_W & \sin \theta_W \\ 0 & -\sin \theta_W & \cos \theta_W \end{pmatrix}, \quad (5.5)$$

where $\theta_V, \theta_W \in [0, \pi/2)$ is the physical range for the mixing angles and θ_W must not be confused with the weak-mixing ('Weinberg') angle. Before, we assumed $\mu - \tau$ mixing, and

proceed similarly for the evaluation of processes with $\tau - e$ transitions (analogous mixings, in the top left 2×2 submatrix, can be used for quark contributions to $\mu \rightarrow e$ conversion in nuclei).

We will assume no extra quark mixing and degenerate heavy quarks, then $V_{H\ell}^q$ and W^q will be the identity. Therefore, the other free parameter are: θ_V , θ_W and neutral couplings of heavy Majorana neutrinos: $(\theta S\theta^\dagger)_{\mu\tau}$.

For the form factors we do a consistent expansion on the squared transfer momenta over the squared masses of heavy particles Q^2/λ^2 being $\lambda = \{M_{W_H}, M_{Z_H}, M_{A_H}, M_\Phi, M_i\}$. This amounts to an expansion, at the largest, in the m_τ^2/M_Z^2 ratio.

For completeness and for the interest of the first one on its own, we include two analyses: first we do not assume heavy Majorana neutrinos contributions (this, within the LHT, was not considered before in the literature) and the second case adds the presence of these neutrinos arising from the Inverse See Saw mechanism, as seen in previous sections.

5.1 $\tau \rightarrow \ell P$ ($\ell = e, \mu$)

We begin the discussion of results with the case without Majorana neutrinos. These processes are computed in a single Monte Carlo simulation which runs them simultaneously. The resulting values obtained from our analysis are shown in Table 1. During all Monte Carlo simulations of our analysis each branching ratio has been delimited considering its C.L. with aid of SpaceMath package [75].

| $\tau \rightarrow \ell P$ ($\ell = e, \mu$) (C.L. = 90%) without Majorana neutrinos contribution. | | | |
|---|-----------------------|---|--------|
| New physics (NP) scale (TeV) | | Mixing angles | |
| f | 1.49 | θ_V | 42.78° |
| Branching ratio | | θ_W | 42.69° |
| $\text{Br}(\tau \rightarrow e\pi^0)$ | 5.24×10^{-9} | Masses of partner leptons ($m_{\nu^c} = m_{\ell^c}$)(TeV) | |
| $\text{Br}(\tau \rightarrow \mu\pi^0)$ | 3.42×10^{-9} | $m_{\nu_1^c}$ | 3.12 |
| $\text{Br}(\tau \rightarrow e\eta)$ | 2.32×10^{-9} | $m_{\nu_2^c}$ | 3.15 |
| $\text{Br}(\tau \rightarrow \mu\eta)$ | 1.91×10^{-9} | $m_{\nu_3^c}$ | 3.37 |
| $\text{Br}(\tau \rightarrow e\eta')$ | 2.20×10^{-8} | Masses of partner quarks ($m_{u^c} = m_{d^c}$) (TeV) | |
| $\text{Br}(\tau \rightarrow \mu\eta')$ | 1.79×10^{-8} | $m_{u_i^c}$ | 3.55 |
| Masses of T-odd leptons (TeV) | | | |
| $m_{\ell_H^1}$ | 2.11 | | |
| $m_{\ell_H^2}$ | 2.11 | | |
| $m_{\ell_H^3}$ | 2.12 | | |
| $m_{\nu_H^1}$ | 2.10 | | |
| $m_{\nu_H^2}$ | 2.11 | | |
| $m_{\nu_H^3}$ | 2.11 | | |
| Masses of T-odd quarks (TeV) | | | |
| $m_{d_H^i}$ | 2.71 | | |
| $m_{u_H^i}$ | 2.70 | | |

Table 1. Mean values for branching ratios, masses of LHT heavy particles, and mixing angles obtained by Monte Carlo simulation of $\tau \rightarrow \ell P$ ($\ell = e, \mu$) processes where Majorana neutrinos contribution is not considered.

We observe that T-odd leptons are lighter than T-odd quarks by 0.6 TeV which means that $|\kappa_{ii}| < |\kappa_{ii}^q|$, that is, the Yukawa couplings of T-odd quarks are more intense ($|\kappa_{ii}| < 1.002$ and $|\kappa_{ii}^q| < 1.282$). We recall that in our model we are considering degenerate T-odd quarks for simplicity.

Regarding partner leptons ($m_{\nu_i^c}$) and partner quarks ($m_{u_i^c}$) their masses are above 3 TeV, being the latter the heaviest particles coming from LHT.

The mean values for mixing angles θ_V and θ_W are 42.78° and 42.69° , that is $\theta_V \approx \theta_W \approx \pi/4.2$. This result is close to maximize the LFV effects, since this happens when $\theta_V = \theta_W = \pi/4$.

In Figures 6 and 7 the correlations among branching ratios and their free parameters are shown for decay modes with $\ell = e$ and $\ell = \mu$, respectively. We want to highlight the free parameters that have sizeable correlations among them. The magnitude of Yukawa couplings for T-odd leptons is anticorrelated with the T-odd quark ones. This is related to the T-odd leptons being lighter than T-odd quarks. On the other hand, the correlations among the Yukawa couplings of T-odd leptons are high, which results in their masses being very similar.

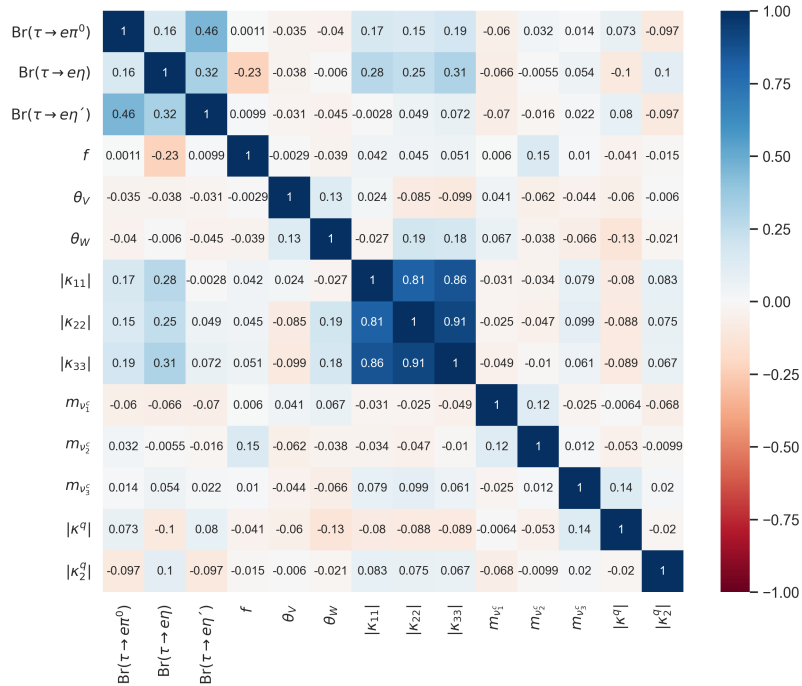


Figure 6. Heat map showing little correlation among $\tau \rightarrow eP$ decays and their free parameters (case without Majorana neutrinos).

In Figures 8 and 9 we see how the branching ratios for both decay modes behave versus f . In both scatter plots the decay mode with $P = \eta'$ reaches the highest values, meanwhile the $P = \eta$ channel is the most restricted one.

The mean values of branching ratios from our numerical analysis are one (η' modes) or at most two orders of magnitude smaller than the current ones [11], which is quite promising

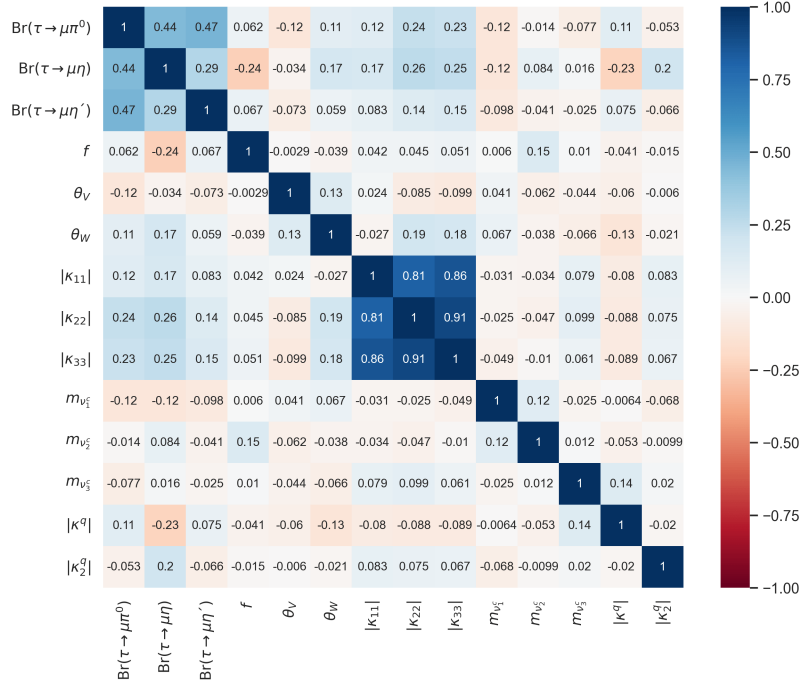


Figure 7. Heat map for $\tau \rightarrow \mu P$ decays and their free parameters, where we see a similar behavior to $\tau \rightarrow e P$ decays (case without Majorana neutrinos).

recalling that we considered only particles from LHT in this analysis.

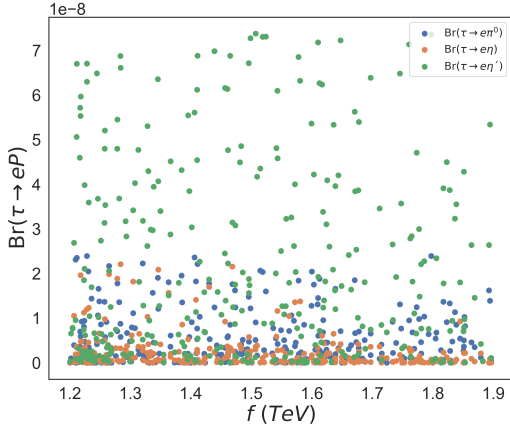


Figure 8. Scatter plot f vs. $\text{Br}(\tau \rightarrow e P)$ without Majorana neutrinos.

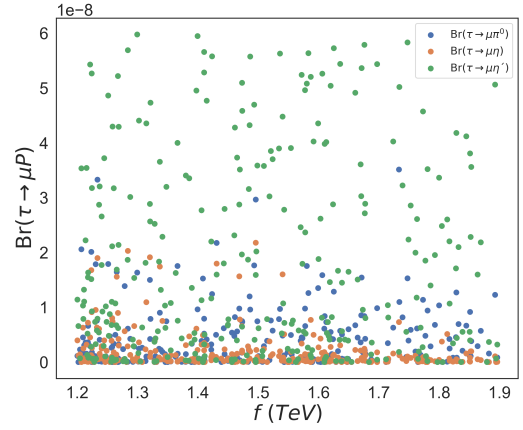


Figure 9. Scatter plot f vs. $\text{Br}(\tau \rightarrow \mu P)$ without Majorana neutrinos.

Now we include the contribution from Majorana neutrinos. Then, the decays can be distinguished by their neutral couplings: $(\theta S \theta^\dagger)_{e\tau}$ -processes and $(\theta S \theta^\dagger)_{\mu\tau}$ -processes. Both types of decays share almost the same free parameters just differing by the neutral couplings of heavy Majorana neutrinos. Therefore, the phenomenological analysis for $\tau \rightarrow$

| $\tau \rightarrow \ell P$ ($\ell = e, \mu$) (C.L. = 90%) with Majorana neutrinos contribution. | | | |
|--|-----------------------|---|-----------------------|
| New physics (NP) scale (TeV) | | Mixing angles | |
| f | 1.51 | θ_V | 43.07° |
| Branching ratio | | θ_W | 42.82° |
| $\text{Br}(\tau \rightarrow e\pi^0)$ | 8.69×10^{-9} | Masses of partner leptons ($m_{\nu^c} = m_{\ell^c}$)(TeV) | |
| $\text{Br}(\tau \rightarrow \mu\pi^0)$ | 6.96×10^{-9} | $m_{\nu_1^c}$ | 3.26 |
| $\text{Br}(\tau \rightarrow e\eta)$ | 6.19×10^{-9} | $m_{\nu_2^c}$ | 3.26 |
| $\text{Br}(\tau \rightarrow \mu\eta)$ | 5.19×10^{-9} | $m_{\nu_3^c}$ | 3.30 |
| $\text{Br}(\tau \rightarrow e\eta')$ | 2.19×10^{-8} | Masses of partner quarks ($m_{u^c} = m_{d^c}$) (TeV) | |
| $\text{Br}(\tau \rightarrow \mu\eta')$ | 1.94×10^{-8} | m_{u^c} | 3.31 |
| Masses of T-odd leptons (TeV) | | Masses of heavy Majorana neutrinos (TeV) | |
| $m_{\ell_H^1}$ | 3.06 | M_1 | 19.18 |
| $m_{\ell_H^2}$ | 3.03 | M_2 | 19.07 |
| $m_{\ell_H^3}$ | 3.03 | M_3 | 19.25 |
| $m_{\nu_H^1}$ | 3.05 | Neutral couplings of heavy Majorana neutrinos | |
| $m_{\nu_H^2}$ | 3.02 | $ (\theta S\theta^\dagger)_{e\tau} $ | 3.32×10^{-7} |
| $m_{\nu_H^3}$ | 3.02 | $ (\theta S\theta^\dagger)_{\mu\tau} $ | 3.90×10^{-7} |
| Masses of T-odd quarks (TeV) | | | |
| $m_{d_H^i}$ | 2.78 | | |
| $m_{u_H^i}$ | 2.78 | | |

Table 2. Mean values for branching ratios, masses of LHT heavy particles, mixing angles and neutral couplings obtained by Monte Carlo simulation of $\tau \rightarrow \ell P$ ($\ell = e, \mu$) processes (case with Majorana neutrinos).

ℓP ($\ell = e, \mu$) decays is done through a single Monte Carlo simulation in which the six decays are run simultaneously. In Table 2 the corresponding analysis results are shown.

In this case, with heavy Majorana neutrinos contribution, the new physics (NP) scale is slightly larger (~ 0.02 TeV) than without them. Now T-odd leptons are heavier than before by ~ 0.09 TeV, but the T-odd quarks keep basically the same values. Actually, here the mass ordering between T-odd leptons and quarks ($m_{(\ell,\nu)_H^i} > m_{(d,u)_H^i}$) is reversed with respect to our first analysis, without Majorana neutrinos.

The partner particles behavior is different than the T-odd ones. Within partner particles, quarks are heavier than leptons. The presence of Majorana neutrinos causes the partner leptons have very similar masses to partner quarks.

The new values that appear in this analysis are the masses of heavy Majorana neutrinos and their neutral couplings. We observe that the masses of Majorana neutrinos are above 19 TeV, being the maximum difference among them ~ 0.18 TeV. Their neutral couplings for both processes have the same order of magnitude, $\sim \mathcal{O}(10^{-7})$, in agreement with our previous paper [52].

In the following two heatmaps, Figures 10 and 11, branching ratios are almost uncorrelated with their free parameters.

The relation among Yukawa couplings of T-odd leptons and quarks is kept from the previous case, without Majorana neutrinos. Likewise, the high correlation among Yukawa couplings of T-odd leptons continues when Majorana neutrinos are added.

The way the branching ratios are correlated in this analysis looks different than the

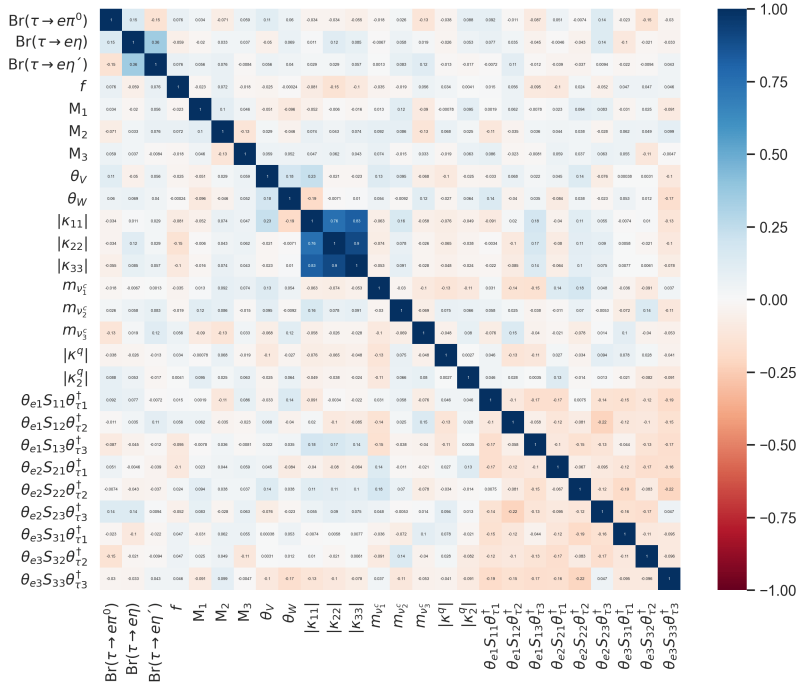


Figure 10. Heat map showing absence of sizable correlations among $\tau \rightarrow eP$ decays and their free parameters (case with Majorana neutrinos).

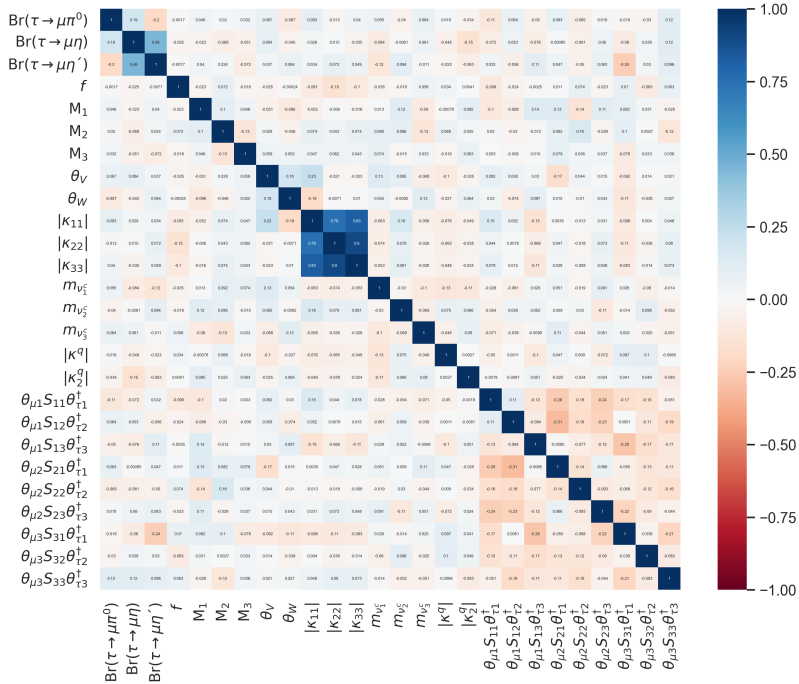


Figure 11. Heat map for $\tau \rightarrow \mu P$ decays and their free parameters, where we see a similar behavior to $\tau \rightarrow eP$ decays (case with Majorana neutrinos).

case without Majorana neutrinos. For both processes with $\ell = e$ and $\ell = \mu$ considering Majorana neutrinos contribution, the decay modes with $P = \eta$ and $P = \eta'$ have the highest correlations. To explain that, we need to get back to eqs. (4.41) and (4.46) and see that their a_P^k and b_P^k factors look similar in these cases.

In contrast to our previous analysis [52], here the heavy Majorana neutrinos are barely correlated among them. In Ref. [52], the mean value for heavy Majorana masses is around 17.2 TeV, differing slightly ($\sim 0.12\%$) in all cases. In this analysis this mean value is ~ 19.2 TeV. Thus, the difference between both studies is just $\sim 10\%$.

The mean values for mixing angles θ_V and θ_W are 43.07° and 42.82° , respectively. This is $\theta_V \approx \theta_W \approx \pi/4.18$, close to maximize the LFV effects, which happens when $\theta_V = \theta_W = \pi/4$.

The two neutral couplings $|(\theta S \theta^\dagger)_{\ell\tau}|$ ($\ell = e, \mu$) have the same order of magnitude, $\mathcal{O}(10^{-7})$, which matches the values reported in [52].

The interpretation of the following Figures 12, 13, 14 and 15 is analogous to the case without Majorana neutrinos contributions, but now we include the correlation between branching ratio versus masses of Majorana neutrinos, that looks similar to the branching ratios with respect to f plots. This is reasonable, as f and M_i are correlated for the consistency of the model.

Our branching ratios are slightly larger when the Majorana neutrinos contribution is included. Again, results are more promising for the $\tau \rightarrow \ell\eta'$ modes, which are only one order of magnitude smaller (at most two, in other decay channels) than current upper limits [11].

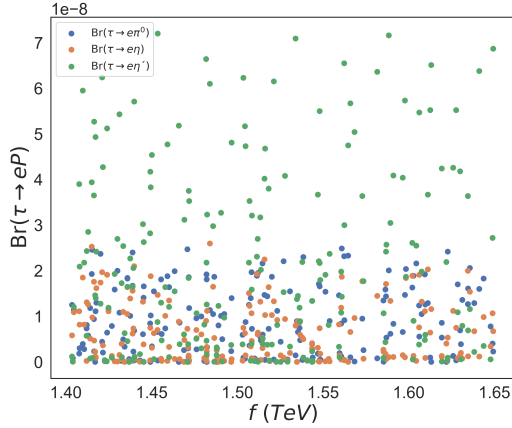


Figure 12. Scatter plot f vs. $\text{Br}(\tau \rightarrow eP)$ considering Majorana neutrinos.

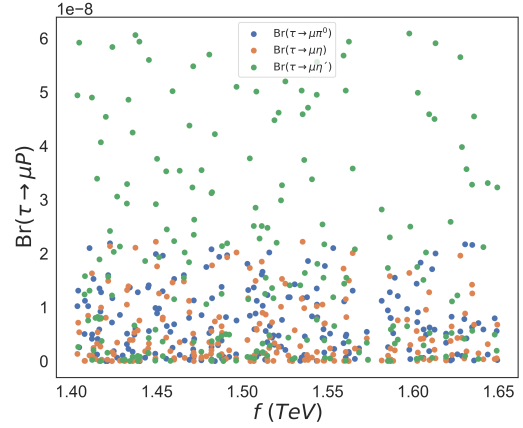


Figure 13. Scatter plot f vs. $\text{Br}(\tau \rightarrow \mu P)$ considering Majorana neutrinos.

5.2 $\tau \rightarrow \ell PP, \ell V$ ($\ell = e, \mu$)

Because the structure of the branching ratios for the processes $\tau \rightarrow \ell PP$ and $\tau \rightarrow \ell V$ ($\ell = e, \mu$) is very similar, they have been computed simultaneously by a single Monte Carlo simulation. We can see the obtained results for this analysis in Tables 3 and 4, where two

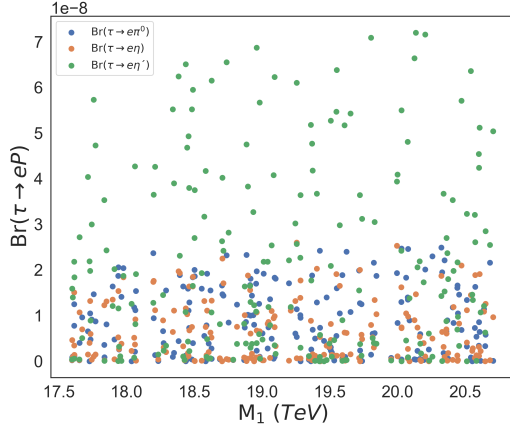


Figure 14. Scatter plot M_1 vs. $\text{Br}(\tau \rightarrow eP)$ considering Majorana neutrinos.

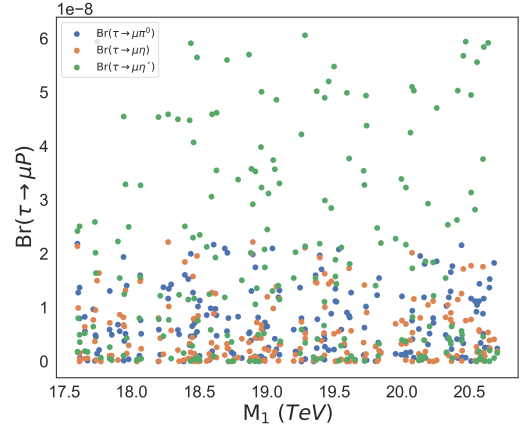


Figure 15. Scatter plot M_1 vs. $\text{Br}(\tau \rightarrow \mu P)$ considering Majorana neutrinos.

cases have been handled: firstly when only particles coming from the LHT are involved in the processes (table 3). Second, adding the effects of Majorana neutrinos (table 4).

| $\tau \rightarrow \ell PP, \ell V$ ($\ell = e, \mu$) (C.L. = 90%) without Majorana neutrinos contribution | | | |
|---|-----------------------|---|---------------|
| New physics (NP) scale (TeV) | | Mixing angles | |
| f | 1.50 | θ_V | 43.36° |
| Branching ratio | | θ_W | 41.50° |
| $\text{Br}(\tau \rightarrow e\pi^+\pi^-)$ | 3.92×10^{-9} | Masses of partner leptons ($m_{\nu^c} = m_{\ell^c}$)(TeV) | |
| $\text{Br}(\tau \rightarrow \mu\pi^+\pi^-)$ | 3.96×10^{-9} | $m_{\nu_1^c}$ | 3.20 |
| $\text{Br}(\tau \rightarrow eK^+K^-)$ | 2.38×10^{-9} | $m_{\nu_2^c}$ | 3.15 |
| $\text{Br}(\tau \rightarrow \mu K^+K^-)$ | 2.85×10^{-9} | $m_{\nu_3^c}$ | 3.31 |
| $\text{Br}(\tau \rightarrow eK^0\bar{K}^0)$ | 1.15×10^{-9} | Masses of partner quarks ($m_{u^c} = m_{d^c}$) (TeV) | |
| $\text{Br}(\tau \rightarrow \mu K^0\bar{K}^0)$ | 1.33×10^{-9} | $m_{u_i^c}$ | 3.32 |
| $\text{Br}(\tau \rightarrow e\rho)$ | 1.10×10^{-9} | | |
| $\text{Br}(\tau \rightarrow \mu\rho)$ | 1.12×10^{-9} | | |
| $\text{Br}(\tau \rightarrow e\phi)$ | 1.77×10^{-9} | | |
| $\text{Br}(\tau \rightarrow \mu\phi)$ | 1.87×10^{-9} | | |
| Masses of T-odd leptons (TeV) | | | |
| $m_{\ell_H^1}$ | 3.13 | | |
| $m_{\ell_H^2}$ | 2.99 | | |
| $m_{\ell_H^3}$ | 3.10 | | |
| $m_{\nu_H^1}$ | 3.12 | | |
| $m_{\nu_H^2}$ | 2.98 | | |
| $m_{\nu_H^3}$ | 3.09 | | |
| Masses of T-odd quarks (TeV) | | | |
| $m_{d_H^i}$ | 2.92 | | |
| $m_{u_H^i}$ | 2.91 | | |

Table 3. Mean values for branching ratios, masses of LHT heavy particles, mixing angles and neutral couplings obtained by Monte Carlo simulation of $\tau \rightarrow \ell PP, \ell V$ ($\ell = e, \mu$) processes without Majorana neutrinos.

Addition of Majorana neutrinos increases both the new physics scale (f) and the masses

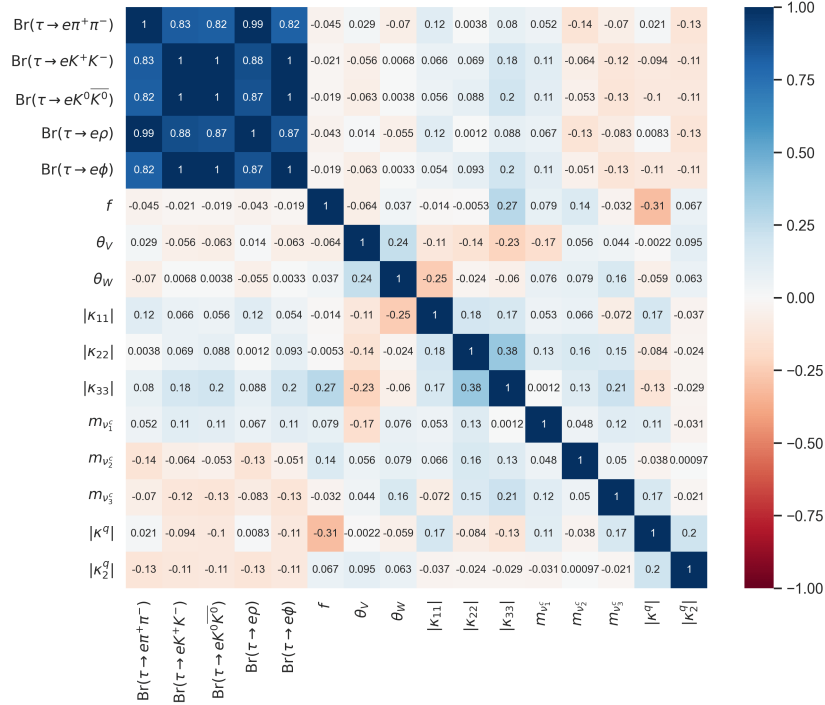


Figure 16. Heat map for $\tau \rightarrow ePP$, eV decays and their free parameters not considering Majorana neutrinos.

of T-odd particles. The NP scale and T-odd lepton masses increase by just ~ 0.05 TeV, whereas the T-odd quark masses grow by ~ 0.8 TeV. The mass ordering of T-odd particles is the same as in $\tau \rightarrow \ell P$ decays, without Majorana neutrinos (i. e., T-odd quarks are heavier). This hierarchy of masses is reversed if Majorana neutrinos are taken into account in $\tau \rightarrow \ell P$ decays, though.

While in Tables 1, 2 and 3, the masses of T-odd quarks do not exceed 3 TeV, in Table 4 they are around 3.7 TeV, which is almost ~ 1 TeV larger than the values obtained in the other three analyses.

In all cases but the $\tau \rightarrow \ell PP$, ℓV processes with Majorana neutrinos, the masses of partner leptons are above 3 TeV. Partner quarks are always heavier than lepton partners. Only in $\tau \rightarrow \ell PP$, ℓV processes with Majorana neutrinos the T-odd particles are heavier than the partner ones.

The values for mixing angles θ_V and θ_W do not have a sizeable difference between this section and the previous one $\sim \pi/4.20$. Again the values tend to maximize the LFV effects.

The Figures 16, 17, 22 and 23 stand for a correlation matrix where we can see how branching ratios and free parameters are correlated.

Correlation among branching ratios for $\tau \rightarrow \ell PP$, ℓV processes look very similar in all cases. This can be understood as a result of the largest contribution coming always from the pions loop in the $F_V^{PP}(s)$ function. This causes the correlations among them to be maximal.

Sizable correlation among Yukawa couplings in the $\tau \rightarrow \ell P$ decays discussed previously,

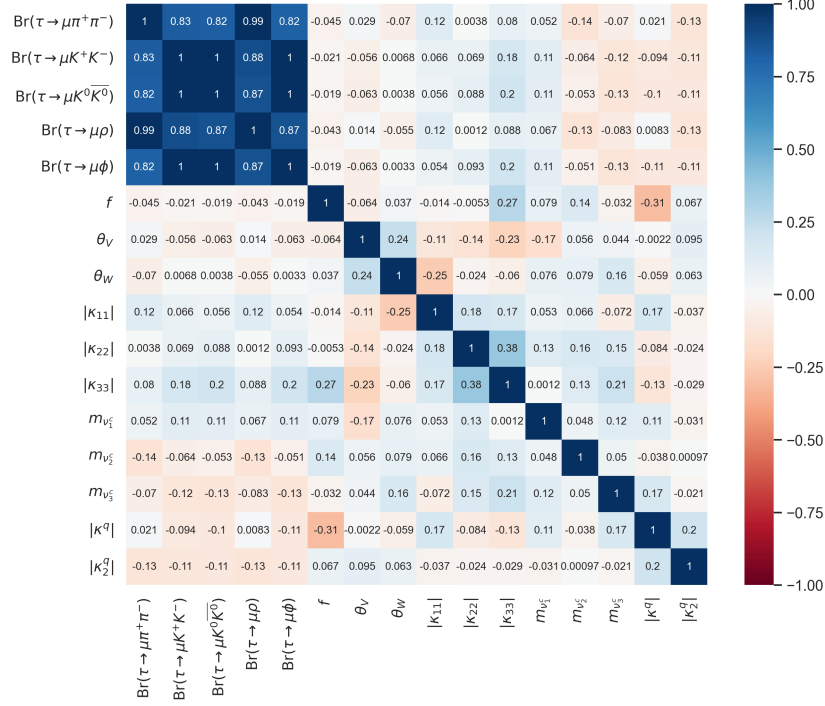


Figure 17. Heat map for $\tau \rightarrow \mu PP$, μV decays and their free parameters, where we see a similar behavior to $\tau \rightarrow e PP$, $e V$ decays not considering Majorana neutrinos.

is not occurring in the PP, V channels. While the masses of T-odd particles in Tables 1 and 2 are very similar, in Tables 3 and 4 the masses of T-odd particles vary clearly.

Magnitudes of neutral couplings in Tables 2 and 4 are of the same order of magnitude. Majorana neutrino masses are slightly lighter in the $\tau \rightarrow \ell PP$, ℓV cases than in the $\tau \rightarrow \ell P$ processes, with all of them being ~ 19 TeV.

Branching ratios for all processes are mildly larger when Majorana neutrinos contribution is included. All our results for $\tau \rightarrow \ell P, PP, V$ ($\ell = e, \mu$) are very promising, as most of them are only one order of magnitude smaller than current bounds [11].

We note that the branching ratios are arranged in triplets in Figures 18 and 19, where the $\pi^+ \pi^-$ mode has the largest probability. Figures 20 and 21 show how the branching ratios for $\tau \rightarrow \ell V$ processes behave with respect to f , where the decay modes with $V = \phi$ as final state reach the highest values.

The interpretation of scatter plots in Figures 24, 25, 26 and 27 is analogous to those without Majorana neutrino, as expected. Additionally, in the case with Majorana neutrinos we can see how branching ratios behave with respect to Majorana neutrino masses M_i in Figures 28, 29, 30 and 31. They look like the scatter plots $\text{Br}(\tau \rightarrow \ell PP(V))$ vs. f , which was expected because both magnitudes are related, $M_i \leq 4\pi f$.

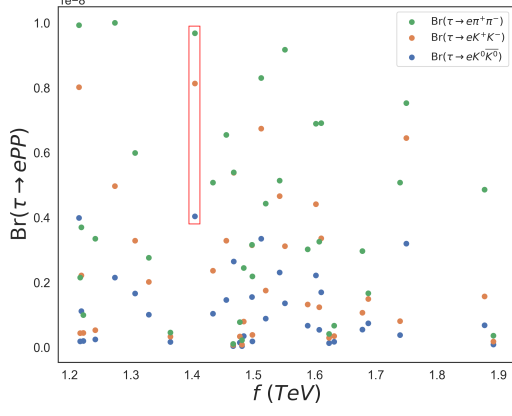


Figure 18. Scatter plot f vs. $\text{Br}(\tau \rightarrow ePP)$ without Majorana neutrinos contribution.

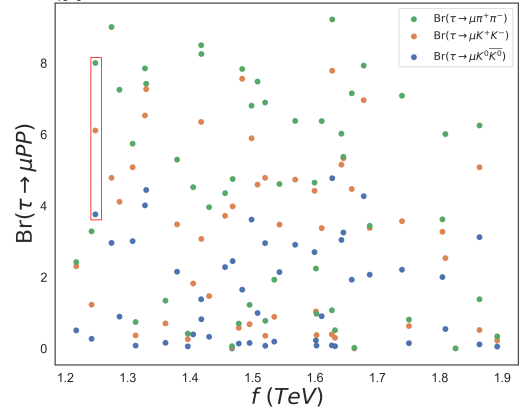


Figure 19. Scatter plot f vs. $\text{Br}(\tau \rightarrow \mu PP)$ without Majorana neutrinos contribution.

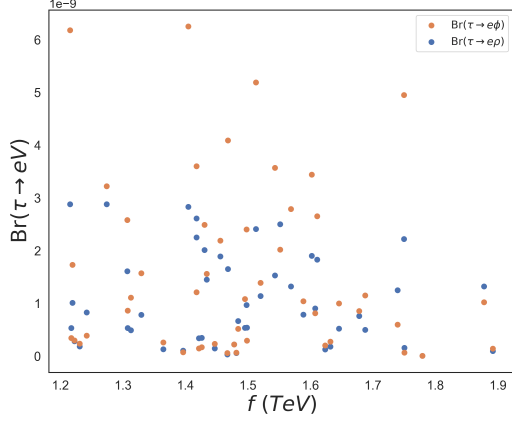


Figure 20. Scatter plot f vs. $\text{Br}(\tau \rightarrow eV)$ without Majorana neutrinos contribution.

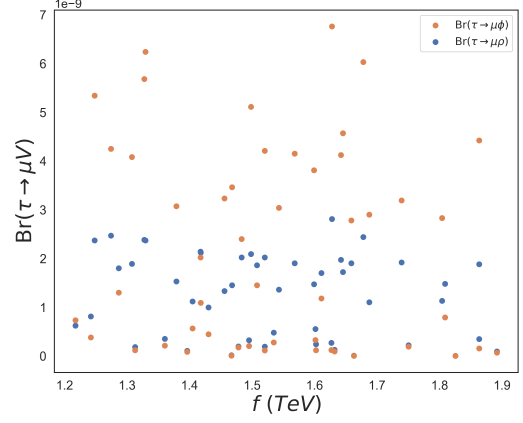


Figure 21. Scatter plot f vs. $\text{Br}(\tau \rightarrow \mu V)$ without Majorana neutrinos contribution.

| $\tau \rightarrow \ell PP, \ell V$ ($\ell = e, \mu$) (C.L. = 90%) with Majorana neutrinos contribution | | | |
|--|-----------------------|---|-----------------------|
| New physics (NP) scale (TeV) | | Mixing angles | |
| f | 1.54 | θ_V | 43.61° |
| Branching ratio | | θ_W | 42.21° |
| $\text{Br}(\tau \rightarrow e\pi^+\pi^-)$ | 4.75×10^{-9} | Masses of partner leptons ($m_{\nu^c} = m_{\ell^c}$)(TeV) | |
| $\text{Br}(\tau \rightarrow \mu\pi^+\pi^-)$ | 4.90×10^{-9} | $m_{\nu_1^c}$ | 2.91 |
| $\text{Br}(\tau \rightarrow eK^+K^-)$ | 2.53×10^{-9} | $m_{\nu_2^c}$ | 2.99 |
| $\text{Br}(\tau \rightarrow \mu K^+K^-)$ | 3.38×10^{-9} | $m_{\nu_3^c}$ | 2.95 |
| $\text{Br}(\tau \rightarrow eK^0\bar{K}^0)$ | 1.16×10^{-9} | Masses of partner quarks ($m_{u^c} = m_{d^c}$) (TeV) | |
| $\text{Br}(\tau \rightarrow \mu K^0\bar{K}^0)$ | 1.50×10^{-9} | $m_{u_i^c}$ | 3.08 |
| $\text{Br}(\tau \rightarrow e\rho)$ | 1.33×10^{-9} | Masses of heavy Majorana neutrinos (TeV) | |
| $\text{Br}(\tau \rightarrow \mu\rho)$ | 1.39×10^{-9} | M_1 | 18.82 |
| $\text{Br}(\tau \rightarrow e\phi)$ | 1.78×10^{-9} | M_2 | 19.33 |
| $\text{Br}(\tau \rightarrow \mu\phi)$ | 2.08×10^{-9} | M_3 | 18.92 |
| Masses of T-odd leptons (TeV) | | Neutral couplings of heavy Majorana neutrinos | |
| $m_{\ell_H^1}$ | 3.49 | $ (\theta S\theta^\dagger)_{e\tau} $ | 2.20×10^{-7} |
| $m_{\ell_H^2}$ | 3.47 | $ (\theta S\theta^\dagger)_{\mu\tau} $ | 3.14×10^{-7} |
| $m_{\ell_H^3}$ | 3.21 | | |
| $m_{\nu_H^1}$ | 3.48 | | |
| $m_{\nu_H^2}$ | 3.46 | | |
| $m_{\nu_H^3}$ | 3.20 | | |
| Masses of T-odd quarks (TeV) | | | |
| $m_{d_H^i}$ | 3.73 | | |
| $m_{u_H^i}$ | 3.71 | | |

Table 4. Mean values for branching ratios, masses of LHT heavy particles, mixing angles and neutral couplings obtained by Monte Carlo simulation of $\tau \rightarrow \ell PP, \ell V$ ($\ell = e, \mu$) processes.

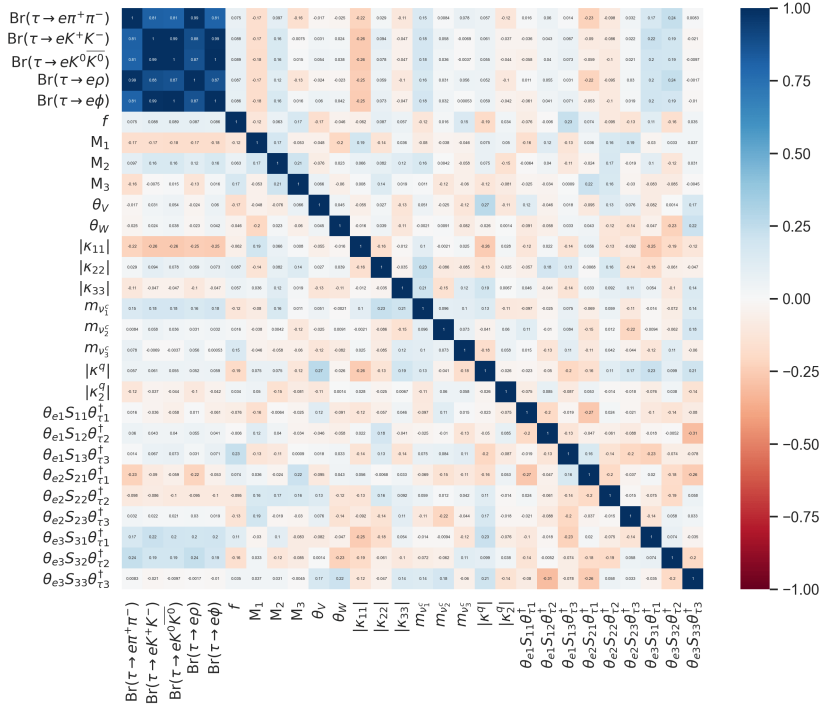


Figure 22. Heat map for $\tau \rightarrow ePP$, eV decays and their free parameters considering Majorana neutrinos.

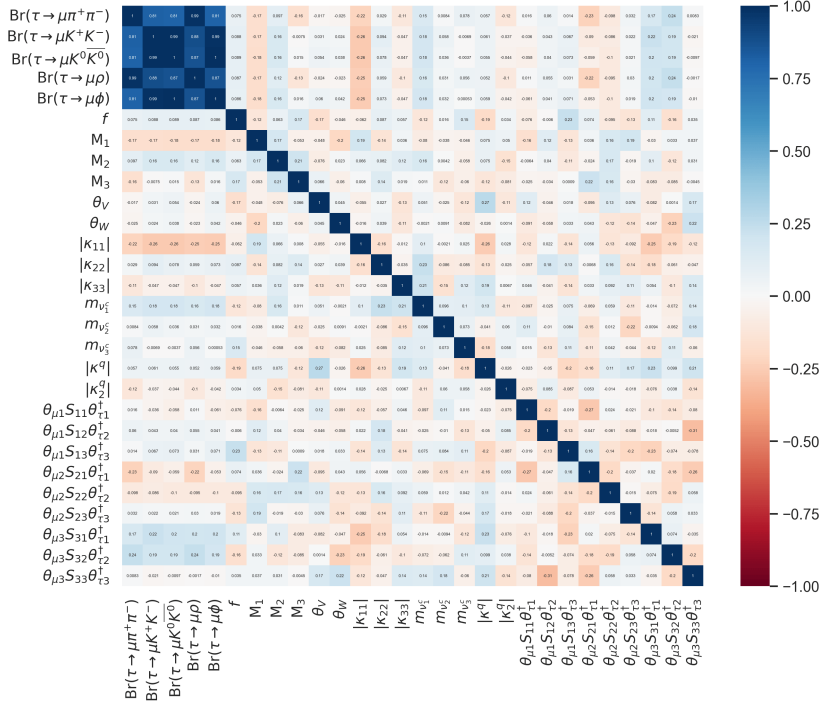


Figure 23. Heat map for $\tau \rightarrow \mu PP$, μV decays and their free parameters, where we see a similar behavior to $\tau \rightarrow ePP$, eV decays considering Majorana neutrinos.

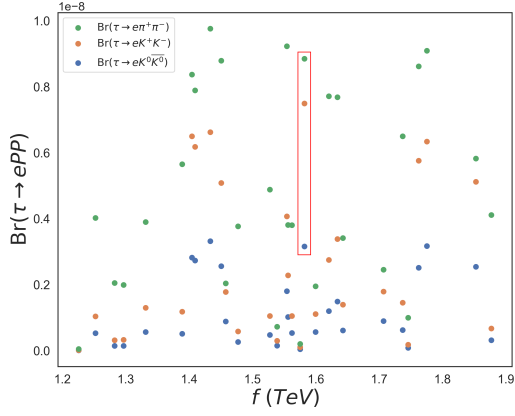


Figure 24. Scatter plot f vs. $\text{Br}(\tau \rightarrow ePP)$ considering Majorana neutrinos.

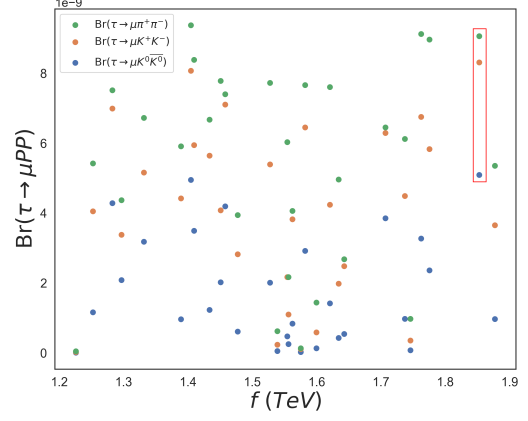


Figure 25. Scatter plot f vs. $\text{Br}(\tau \rightarrow \mu PP)$ considering Majorana neutrinos.

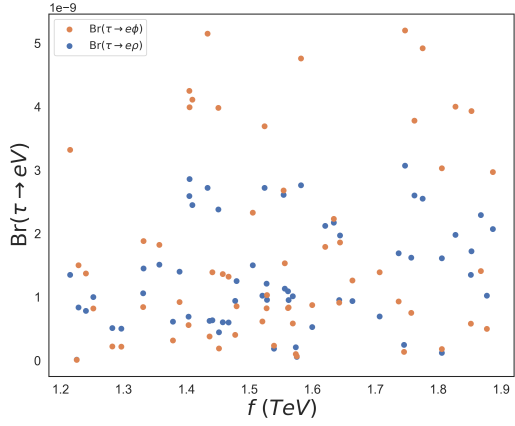


Figure 26. Scatter plot f vs. $\text{Br}(\tau \rightarrow eV)$ considering Majorana neutrinos.

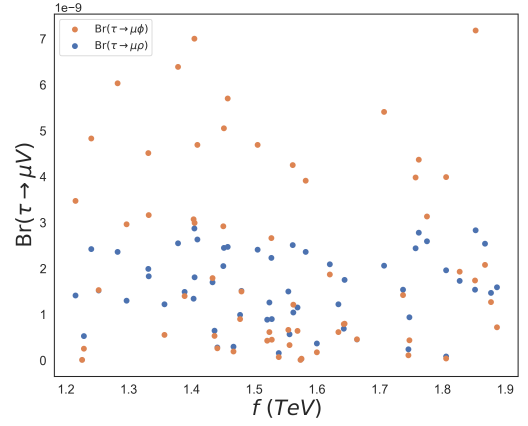


Figure 27. Scatter plot f vs. $\text{Br}(\tau \rightarrow \mu V)$ considering Majorana neutrinos.

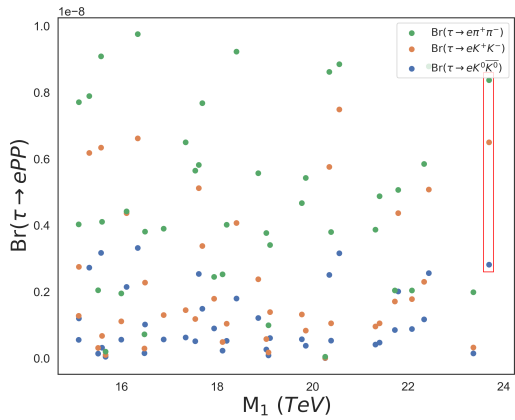


Figure 28. Scatter plot M_1 vs. $\text{Br}(\tau \rightarrow ePP)$ considering Majorana neutrinos.

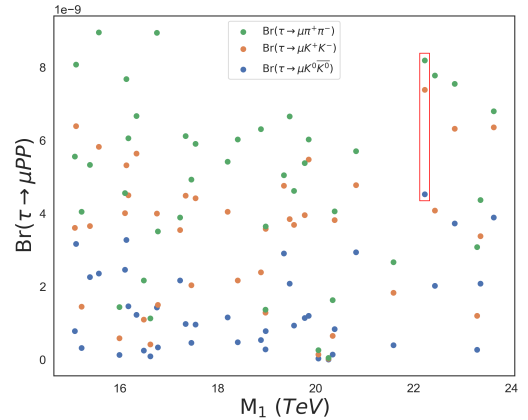


Figure 29. Scatter plot M_1 vs. $\text{Br}(\tau \rightarrow \mu PP)$ considering Majorana neutrinos.

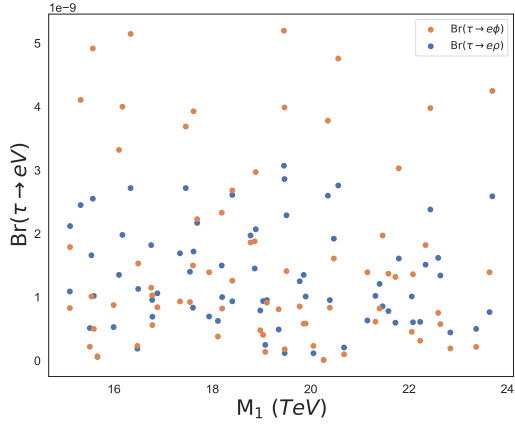


Figure 30. Scatter plot M_1 vs. $\text{Br}(\tau \rightarrow eV)$ considering Majorana neutrinos.

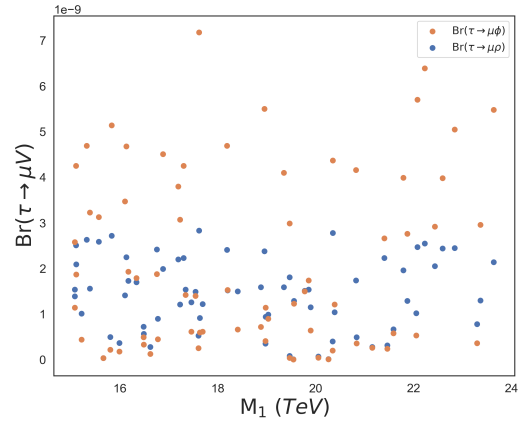


Figure 31. Scatter plot M_1 vs. $\text{Br}(\tau \rightarrow \mu V)$ considering Majorana neutrinos.

6 Conclusions

Although LFV processes have been studied extensively within the LHT model, an analysis of semileptonic tau decays was still lacking. We have tackled it here, both considering only effects of T -odd and partner fermions, and also adding the contributions from Majorana neutrinos realizing an inverse seesaw mechanism of type I. Our main results are summarized in the following:

- Masses of particles coming from LHT, T -odd and partner fermions, are below 4 TeV, almost 5 times lighter than heavy Majorana neutrinos. This is consistent with the next item.
- The new physics (NP) scale is around $f \sim 1.5$ TeV, which is accompanied by heavy Majorana neutrinos with $M_i \sim 19$ TeV (we recall that $M_i \sim 4\pi f$). Compared to our previous work [52], these masses of heavy Majorana neutrinos are heavier by ~ 2 TeV ($\sim 10\%$ of difference) and f is fully consistent.
- The magnitudes of neutral couplings of heavy Majorana neutrinos $|(\theta S \theta^\dagger)_{\ell\tau}|$ ($\ell = e, \mu$) match those reported in [52].
- The masses of T -odd particles from $\tau \rightarrow \ell P$ processes differ from those in the $\tau \rightarrow \ell PP, \ell V$ ($\ell = e, \mu$) decays by ~ 1 TeV. All other mean values from Tables 1, 2, 3 and 4 agree. Taking this into account, we consider these values as representative for the present analysis of our model. A global analyses (including purely leptonic processes and conversions in nuclei) is required, however, and will be presented elsewhere.
- All our results are very promising and will be probed in future measurements, as they lie approximately only one order of magnitude below current bounds [11].

Acknowledgements

We are indebted to Jorge Portolés for useful discussions. I. P. acknowledges Conacyt funding his Ph. D and P. R. the financial support of Cátedras Marcos Moshinsky (Fundación Marcos Moshinsky) and Conacyt's project within 'Paradigmas y Controversias de la Ciencia 2022', number 319395.

A Appendix: Form Factor Functions of T-odd Contribution

The functions involved in the F_M^γ form factor of T-odd contributions are (we omit their second argument, which is always Q^2 , below)

$$\begin{aligned}
F_{Z_H}(y) &= -\frac{1}{3} + \frac{2y + 5y^2 - y^3}{8(1-y)^3} + \frac{3y^2}{4(1-y)^4} \ln y \\
&\quad + \frac{1}{48} \frac{Q^2}{M_{Z_H}^2} \left(\frac{24 + 546y - 2479y^2 + 561y^3 - 339y^4 + 67y^5}{60(1-y)^5} + \frac{y(6 - 17y - 16y^2) \ln y}{(1-y)^6} \right), \\
F_{W_H}(y) &= \frac{5}{6} - \frac{3y - 15y^2 - 6y^3}{12(1-y)^3} + \frac{3y^3}{2(1-y)^4} \ln y \\
&\quad + \frac{y}{24} \frac{Q^2}{M_{W_H}^2} \left(\frac{134 - 759y + 1941y^2 - 2879y^3 - 69y^4 + 12x^5}{60(1-y)^5} + \frac{y^3(4 - 34y + 3y^3) \ln y}{(1-y)^6} \right), \\
F_{\bar{\nu}^c}(x) &= \frac{-1 + 5x + 2x^2}{12(1-x)^3} + \frac{x^2}{2(1-x)^4} \ln x \\
&\quad + \frac{x^2}{24} \frac{Q^2}{M_\Phi^2} \left(\frac{13 - 87x + 333x^2 + 293x^3 - 12x^4}{60(1-x)^5} + \frac{x^3(8+x) \ln x}{(1-x)^6} \right), \\
F_{\bar{\ell}^c}(x) &= \frac{-4 + 5x + 5x^2}{6(1-x)^3} - \frac{x(1-2x)}{(1-x)^4} \ln x \\
&\quad + \frac{1}{8} \frac{Q^2}{M_\Phi^2} \left(\frac{4 + 129x - 231x^2 - 91x^3 + 9x^4}{60(1-x)^5} + \frac{x(1-4x^2) \ln x}{(1-x)^6} \right),
\end{aligned} \tag{A.1}$$

with $y_i = \frac{m_{H_i}^2}{M_{W_H}^2}$ being $m_{H_i} \equiv m_{\ell_H^i} \simeq m_{\nu_H^i}$, $a = \frac{M_{W_H}^2}{M_{A_H}^2} = \frac{5c_W^2}{s_W^2} \sim 15$, $M_{W_H} = M_{Z_H}$, and $x_j = \frac{m_{\nu_j^c}^2}{M_\Phi^2}$. We have used $M_W^2/M_{W_H}^2 = v^2/(4f^2)$.

In turn, the functions from eq. (4.6) read

$$\begin{aligned}
G_Z^{(1)}(y) &= \frac{1}{36} + \frac{y(18 - 11y - y^2)}{48(1-y)^3} - \frac{4 - 16y + 9y^2}{24(1-y)^4} \ln y, \\
G_W^{(1)}(y) &= -\frac{5}{18} + \frac{y(12 + y - 7y^2)}{24(1-y)^3} + \frac{y^2(12 - 10y + y^2)}{12(1-y)^4} \ln y, \\
G_{\bar{\nu}^c}^{(1)}(x) &= \frac{2 - 7x + 11x^2}{72(1-x)^3} + \frac{x^3}{12(1-x)^4} \ln x, \\
G_{\bar{\ell}^c}^{(1)}(x) &= \frac{20 - 43x + 29x^2}{36(1-x)^3} + \frac{2 - 3x + 2x^3}{6(1-x)^4} \ln x.
\end{aligned} \tag{A.2}$$

with $y_i = \frac{m_{H_i}^2}{M_{W_H}^2}$, $x_i = \frac{m_{\nu_i^c}^2}{M_{W_H}^2}$ and $a = \frac{5c_W^2}{s_W^2}$.

Form factor functions of F_L^Z are

$$\begin{aligned}
H_L^{W(0)}(y) &= \frac{6-y}{1-y} + \frac{2+3y}{(1-y)^2} \ln y, \\
H_L^W(y) &= 2G_Z^{(1)}(y) - 2c_W^2 G_W^{(1)}(y), \\
H_L^{A/Z}(y) &= G_Z^{(1)}(y), \\
H_L^{\bar{\nu}}(x) &= \frac{1}{2} G_{\bar{\ell}^c}^{(1)}(x) - 2c_W^2 G_{\bar{\nu}^c}^{(1)}(x), \\
H_L^{\bar{\ell}}(x) &= G_{\bar{\ell}^c}^{(1)}(x),
\end{aligned} \tag{A.3}$$

being $y_i = m_{Hi}^2/M_{W_H}^2$ and $y_i = m_{\bar{\nu}_i}^2/M_\Phi^2$. The expression for $G_Z^{(1)}$, $G_W^{(1)}$, $G_{\bar{\nu}^c}^{(1)}$ and $G_{\bar{\ell}^c}^{(1)}$ can be consulted from eq. (A.2).

The four-point functions that appear in the box form factor, in the terms of the mass ratios $x = m_1^2/m_0^2$, $y = m_2^2/m_0^2$, $z = m_3^2/m_0^2$, turn out to be

$$d_0(x, y, z) \equiv m_0^4 D_0 = \left[\frac{x \ln x}{(1-x)(x-y)(x-z)} - \frac{y \ln y}{(1-y)(x-y)(y-z)} + \frac{z \ln z}{(1-z)(x-z)(y-z)} \right], \tag{A.4}$$

$$\bar{d}_0(x, y, z) \equiv 4m_0^2 D_{00} = \left[\frac{x^2 \ln x}{(1-x)(x-y)(x-z)} - \frac{y^2 \ln y}{(1-y)(x-y)(y-z)} + \frac{z^2 \ln z}{(1-z)(x-z)(y-z)} \right], \tag{A.5}$$

$$\bar{d}'_0(x, y, z) = \frac{x^2 \ln x}{(1-x)(x-y)(z-x)} + \frac{y^2 \ln y}{(1-y)(x-y)(z-y)} + \frac{z^2 \ln z}{(1-z)(x-z)(y-z)}, \tag{A.6}$$

with $\bar{d}(x, y) = \bar{d}'(x, y, 1)$. For two equals masses ($m_0 = m_3$) we get

$$d_0(x, y) = - \left[\frac{x \ln x}{(1-x)^2(x-y)} - \frac{y \ln y}{(1-y)^2(x-y)} + \frac{1}{(1-x)(1-y)} \right], \tag{A.7}$$

$$\bar{d}_0(x, y) = - \left[\frac{x^2 \ln x}{(1-x)^2(x-y)} - \frac{y^2 \ln y}{(1-y)^2(x-y)} + \frac{1}{(1-x)(1-y)} \right]. \tag{A.8}$$

B Appendix: Form Factor Functions of Majorana Contribution

The functions that make up the eq. (4.19) are

$$\begin{aligned}
F_M^{\chi^h}(y, Q^2) &= \frac{1}{3} - \frac{2y^3 - 7y^2 + 11y}{4(1-y)^3} + \frac{3y}{2(1-y)^4} \ln y, \\
&\quad - \frac{1}{24} \frac{Q^2}{M_j^2} \left(\frac{134y_j^5 - 759y_j^4 + 1941y_j^3 - 2879y_j^2 - 69y_j + 12}{60y_j(1-y_j)^5} + \frac{(4y_j^2 - 34y_j + 3) \ln y_j}{(1-y_j)^6} \right), \\
F_L^{\chi^h}(y, Q^2) &= 2\Delta_\epsilon + \frac{Q^2}{M_j^2} \left(-\frac{(12y^2 - 10y + 1) \ln y}{6y(1-y)^4} + \frac{20y^3 - 96y^2 + 57y + 1}{36y(1-y)^3} \right),
\end{aligned} \tag{B.1}$$

with $\Delta_\epsilon = \frac{1}{\epsilon} - \gamma_E + \ln(4\pi) + \ln\left(\frac{\mu^2}{M_W^2}\right)$ which regulates the ultraviolet divergence in $4 - 2\epsilon$ dimensions, that is canceled by unitarity of mixing matrices (GIM-like mechanism). The explicit functions F^h , G^h , and H^h are written as follows

$$\begin{aligned} F^h(y_i; Q^2) &\approx -\frac{5}{2} \ln y_i + \frac{Q^2}{M_j^2} \left(\frac{1}{12y_i} (1 - 2s_W^2) \ln y_i \right), \\ G^h(y_i, y_j; M_Z^2) &= \frac{1}{2} \left(\Delta_\epsilon - \frac{1}{2} \right) - \frac{1}{2(y_i - y_j)} \left(-\frac{(1 - y_j) \ln y_i}{(1 - y_i)} + \frac{(1 - y_i) \ln y_j}{(1 - y_j)} \right) + \frac{M_Z^2}{M_j^2} \times (\text{terms}), \\ H^h(y_i, y_j; M_Z^2) &= -\frac{1}{4} \left(\Delta_\epsilon + \frac{1}{2} \right) - \frac{1}{4(y_i - y_j)} \left(-\frac{(1 - 4y_i)y_j \ln y_i}{(1 - y_i)} + \frac{(1 - 4y_j)y_i \ln y_j}{(1 - y_j)} \right) + \frac{M_Z^2}{M_i^2} \times (\text{terms}). \end{aligned} \quad (\text{B.2})$$

where

$$\begin{aligned} G^h(y_i, y_j; Q^2) : (\text{terms}) &= -\frac{1}{12(1 - y_i)^2} \frac{Q^2}{M_j^2} \left(\frac{(1 - y_i)(3(1 + y_j) - 2y_i(2 + 6y_j - y_j^2)) + y_i^2(1 + y_j)}{(y_i - y_j)(1 - y_j)^2} \right. \\ &\quad + \frac{(-6 + y_i(3 + 15y_j - 4y_j^2) + y_i^2(6 - 20y_j - 4y_j^2) + y_i^2(6 - 20y_j + 6y_j^2)) \ln y_j}{(1 - y_j)^3} \\ &\quad \left. + \frac{y_i(3 - 4y_j + 6y_i(1 + y_j) - 12y_i^2) \ln\left(\frac{y_j}{y_i}\right)}{(y_i - y_j)^2} \right), \\ H^h(y_i, y_j; Q^2) : (\text{terms}) &= -\frac{Q^2}{M_i^2} \frac{y_j}{6(1 - y_i)^2} \left(-\frac{y_j(y_i(1 + 3y_j) - (3 + y_j)) \ln y_j}{(1 - y_j)^3} \right. \\ &\quad \left. + \frac{(1 - y_i)((1 - 3y_j - 2y_j^2) - y_i + 5y_i y_j)}{(y_i - y_j)(1 - y_j)^2} + \frac{y_j(1 - 3y_i) \ln\left(\frac{y_j}{y_i}\right)}{(y_i - y_j)^2} \right), \end{aligned} \quad (\text{B.3})$$

with $y_j = \frac{M_W^2}{M_j^2}$, being M_j the masses of heavy Majoranan neutrinos.

The f_{B_d} and f_{B_u} functions yield

$$f_{B_d}(y_i, x_j^u) = \left(1 + \frac{1}{4} \frac{x_j^u}{y_i} \right) \bar{d}_0^{lh}(y_i, x_j^u) - 2 \frac{x_j^u}{y_i} d_0^{lh}(y_i, x_j^u), \quad (\text{B.4})$$

$$f_{B_u}(y_i, x_j^d) = - \left(4 + \frac{x_j^d}{4y_i} \right) \bar{d}_0^{lh}(y_i, x_j^u) + 2 \frac{x_j^u}{y_i} d_0^{lh}(y_i, x_j^u). \quad (\text{B.5})$$

where $d_0^{lh}(y_i, x_j^u)$ and $\bar{d}_0^{lh}(y_i, x_j^u)$ become

$$d_0^{lh}(y_i, x_j^u) = \frac{y_i^2 \ln y_i}{(1 - y_i)^2(1 - y_i x_j^u)} + \frac{x_j^u y_i \ln x_j^u}{(1 - x_j^u)^2(1 - y_i x_j^u)} + \frac{y_i}{(1 - y_i)(1 - x_j^u)}, \quad (\text{B.6})$$

$$\bar{d}_0^{lh}(y_i, x_j^u) = \frac{y_i \ln y_i}{(1 - y_i)^2(1 - y_i x_j^u)} + \frac{y_i (x_j^u)^2 \ln x_j^u}{(1 - x_j^u)^2(1 - y_i x_j^u)} + \frac{y_i}{(1 - y_i)(1 - x_j^u)}, \quad (\text{B.7})$$

with $y_i = M_W^2/M_i^2$ ($i = 1, 2, 3$) and $x_j^u = m_{q_j}^2/M_W^2$ ($j = 1, 2, 3$).

C Appendix: Hadronization tools

Within the R χ T framework, bilinear light quark operators coupled to the external sources are added to the massless QCD Lagrangian:

$$\mathcal{L}_{\text{QCD}} = \mathcal{L}_{\text{QCD}}^0 + \bar{q} [\gamma_\mu (v^\mu + \gamma_5 a^\mu) - (s - ip\gamma_5)] q, \quad (\text{C.1})$$

where the auxiliary fields defined as $v^\mu = v_i^\mu \lambda^i / 2$, $a^\mu = a_i^\mu \lambda^i / 2$, and $s = s_i \lambda^i$, with λ^i the Gell-Mann matrices, are Hermitian matrices in flavour space. Once the R χ T action is fixed through $\mathcal{L}_{\text{R}\chi\text{T}}$, we can hadronize the bilinear quark currents by taking the appropriate functional derivative with respect to the external fields:

$$\begin{aligned} S^i &= -\bar{q} \lambda^i q = \left. \frac{\partial \mathcal{L}_{\text{R}\chi\text{T}}}{\partial s_i} \right|_{j=0}, & P^i &= \bar{q} i \gamma_5 \lambda^i q = \left. \frac{\partial \mathcal{L}_{\text{R}\chi\text{T}}}{\partial p_i} \right|_{j=0}, \\ V_\mu^i &= \bar{q} \gamma_\mu \frac{\lambda^i}{2} q = \left. \frac{\partial \mathcal{L}_{\text{R}\chi\text{T}}}{\partial v_i^\mu} \right|_{j=0}, & A_\mu^i &= \bar{q} \gamma_\mu \gamma_5 \frac{\lambda^i}{2} q = \left. \frac{\partial \mathcal{L}_{\text{R}\chi\text{T}}}{\partial a_i^\mu} \right|_{j=0}, \end{aligned} \quad (\text{C.2})$$

where $j = 0$ indicates that all external currents are set to zero.

The vector form factor from the γ contribution to the decay into two pseudoscalar mesons is driven by the electromagnetic current

$$V_\mu^{\text{em}} = \sum_d^{u,d,s} Q_d \bar{q} \gamma_\mu q = V_\mu^3 + \frac{1}{\sqrt{3}} V_\mu^8 = J_\mu^{\text{em}}, \quad (\text{C.3})$$

where Q_d is the electric charge of the q quark. We get also

$$\begin{aligned} \bar{u} \gamma_\mu P_L u &= J_\mu^3 + \frac{1}{\sqrt{3}} V_\mu^8 + \frac{2}{\sqrt{6}} J_\mu^0, \\ \bar{d} \gamma_\mu P_L d &= -J_\mu^3 + \frac{1}{\sqrt{3}} V_\mu^8 + \frac{2}{\sqrt{6}} J_\mu^0, \\ \bar{s} \gamma_\mu P_L s &= -\frac{2}{\sqrt{3}} V_\mu^8 + \frac{2}{\sqrt{6}} J_\mu^0, \end{aligned} \quad (\text{C.4})$$

where $J_\mu^i = (V_\mu^i - A_\mu^i)/2$. The vector current contributes to an even number of pseudoscalar mesons or a vector resonance, while axial-vector current gives an odd number of pseudoscalar mesons.

In Z contribution both vector and axial-vector currents do contribute:

$$\begin{aligned} J_\mu^Z &= V_\mu^Z + A_\mu^Z, \\ V_\mu^Z &= \frac{g}{2c_W} \bar{q} \gamma_\mu \left[2s_W^2 Q_q - T_3^{(q)} \right] q, \\ A_\mu^Z &= \frac{g}{2c_W} \bar{q} \gamma_\mu \gamma_5 T_3^{(q)} q, \end{aligned} \quad (\text{C.5})$$

with Q_q (see eq. (4.17)) and $T_3^{(q)} = \text{diag}(1, -1, -1)/2$ the electric charge and weak hypercharges, respectively.

C.1 $\tau \rightarrow \mu P$

The $\tau \rightarrow \mu P$ decay, in our model, is mediated only by axial-vector current (Z gauge boson), as \mathcal{M}_γ does not contribute. The total amplitude for $\tau \rightarrow \mu P$ reads

$$\mathcal{M}_{\tau \rightarrow \mu P} = \mathcal{M}_Z^P + \mathcal{M}_{\text{Box}}^P, \quad (\text{C.6})$$

where \mathcal{M}_Z^P is given by

$$\begin{aligned} \mathcal{M}_Z^P &= -i \frac{g^2}{2c_W} \frac{F}{M_Z^2} C(P) \sum_j V_\ell^{j\mu*} V_\ell^{j\tau} \bar{\mu}(p') [\not{Q}(F_L^Z P_L + F_R^Z P_R)] \tau(p), \\ \mathcal{M}_{\text{Box}}^P &= -ig^2 F \sum_j V_\ell^{j\mu*} V_\ell^{j\tau} B_j(P) \bar{\mu}(p') [\not{Q} P_L] \tau(p), \end{aligned} \quad (\text{C.7})$$

where $Z_L = \frac{g}{c_W}(T_3^q - s_W^2 Q_q)$ and $Z_R = -\frac{g}{c_W}s_W^2 Q_q$. The hadronization of the quark bilinear in \mathcal{M}_Z is determined by vector and axial-vector currents from eq. (C.5), which are written in terms of one P meson, turning out to be [69]

$$\begin{aligned} V_\mu^Z &= 0, \\ A_\mu^Z &= -\frac{g}{2c_W} F \{C(\pi^0) \partial_\mu \pi^0 + C(\eta) \partial_\mu \eta + C(\eta') \partial_\mu \eta'\}, \end{aligned} \quad (\text{C.8})$$

where $F \simeq 0.0922$ GeV is the decay constant of the pion and the $C(P)$ functions are given by [62, 69]

$$\begin{aligned} C(\pi^0) &= 1, \\ C(\eta) &= \frac{1}{\sqrt{6}} (\sin \theta_\eta + \sqrt{2} \cos \theta_\eta), \\ C(\eta') &= \frac{1}{\sqrt{6}} (\sqrt{2} \sin \theta_\eta - \cos \theta_\eta). \end{aligned} \quad (\text{C.9})$$

The box amplitude is composed by the following $B_j(P)$ factors [53]

$$\begin{aligned} B_j(\pi^0) &= \frac{1}{2} (B_d^j - B_u^j), \\ B_j(\eta) &= \frac{1}{2\sqrt{3}} [(\sqrt{2} \sin \theta_\eta - \cos \theta_\eta) B_u^j + (2\sqrt{2} \sin \theta_\eta + \cos \theta_\eta) B_d^j], \\ B_j(\eta') &= \frac{1}{2\sqrt{3}} [(\sin \theta_\eta - 2\sqrt{2} \cos \theta_\eta) B_d^j - (\sin \theta_\eta + \sqrt{2} \cos \theta_\eta) B_u^j], \end{aligned} \quad (\text{C.10})$$

where the B_q^j functions are the form factors from box diagrams and the angle $\theta_\eta \simeq -18^\circ$. The branching ratio reads

$$\text{Br}(\tau \rightarrow \mu P) = \frac{1}{4\pi} \frac{\lambda^{1/2}(m_\tau^2, m_\mu^2, m_P^2)}{m_\tau^2 \Gamma_\tau} \frac{1}{2} \sum_{i,f} |\mathcal{M}_{\tau \rightarrow \mu P}|^2, \quad (\text{C.11})$$

where $\Gamma_\tau \approx 2.267 \times 10^{-12}$ GeV and $\lambda(x, y, z) = (x + y - z)^2 - 4xy$, thus $\mathcal{M}_{\tau \rightarrow \mu P}$ is given by eq. (C.6). Thus,

$$\sum_{i,f} |\mathcal{M}_{\tau \rightarrow \mu P}|^2 = \frac{1}{2m_\tau} \sum_{k,l} \left[(m_\tau^2 + m_\mu^2 - m_P^2)(a_P^k a_P^{l*} + b_P^k b_P^{l*}) + 2m_\mu m_\tau (a_P^k a_P^{l*} - b_P^k b_P^{l*}) \right], \quad (\text{C.12})$$

with $k, l = Z, B$. Defining $\Delta_{\tau\mu} = m_\tau - m_\mu$ and $\Sigma_{\tau\mu} = m_\tau + m_\mu$ we get

$$\begin{aligned} a_P^Z &= -\frac{g^2}{2c_W} \frac{F}{2} \frac{C(P)}{M_Z^2} \Delta_{\tau\mu} (F_L^Z + F_R^Z), \\ b_P^Z &= \frac{g^2}{2c_W} \frac{F}{2} \frac{C(P)}{M_Z^2} \Sigma_{\tau\mu} (F_R^Z - F_L^Z), \\ a_P^B &= -\frac{g^2 F}{2} \Delta_{\tau\mu} B_j(P), \\ b_P^B &= -\frac{g^2 F}{2} \Sigma_{\tau\mu} B_j(P). \end{aligned} \quad (\text{C.13})$$

C.2 $\tau \rightarrow \mu PP$

These channels are mediated by γ -, Z -penguins and box diagrams. Using the electromagnetic current (eq. (C.3)), the electromagnetic form factor reads

$$\langle P_1(p_1) P_2(p_2) | V_\mu^{\text{em}} | 0 \rangle = (p_1 - p_2)_\mu F_V^{P_1 P_2}(Q^2), \quad (\text{C.14})$$

where $Q = p_1 + p_2$ and $F_V^{P_1 P_2}(Q^2)$ is steered by both $I = 1$ and $I = 0$ vector resonances. Then, the complete amplitude is given by

$$\mathcal{M}_{\tau \rightarrow \mu PP} = \mathcal{M}_\gamma^{P\bar{P}} + \mathcal{M}_Z^{P\bar{P}} + \mathcal{M}_{\text{Box}}^{P\bar{P}}. \quad (\text{C.15})$$

The next step is to hadronize the quark bilinears appearing in each amplitude. They turn out to be

$$\begin{aligned} \mathcal{M}_\gamma^{P\bar{P}} &= \frac{e^2}{Q^2} F_V^{P_1 P_2}(s) \times \\ &\quad \sum_j V_\ell^{j\mu*} V_\ell^{j\tau} \bar{\mu}(p') [Q^2 (\not{p}_q - \not{p}_{\bar{q}}) F_L^\gamma(Q^2) P_L + 2im_\tau p_q^\mu \sigma_{\mu\nu} p_{\bar{q}}^\nu F_M^\gamma(Q^2) P_R] \tau(p), \\ \mathcal{M}_Z^{P\bar{P}} &= g^2 \frac{2s_W^2 - 1}{2c_W M_Z^2} F_V^{P_1 P_2}(s) \sum_j V_\ell^{j\mu*} V_\ell^{j\tau} \bar{\mu}(p') (\not{p}_q - \not{p}_{\bar{q}}) [\gamma^\mu (F_L^Z P_L + F_R^Z P_R)] \tau(p), \\ \mathcal{M}_{\text{Box}}^{P\bar{P}} &= \frac{g^2}{2} F_V^{P_1 P_2}(s) \sum_j V_\ell^{j\mu*} V_\ell^{j\tau} (B_u^j - B_d^j) \bar{\mu}(p') (\not{p}_q - \not{p}_{\bar{q}}) P_L \tau(p). \end{aligned} \quad (\text{C.16})$$

After computing each amplitude, we get the following branching ratio

$$\text{Br}(\tau \rightarrow \mu PP) = \frac{\kappa_{PP}}{64\pi^3 m_\tau^2 \Gamma_\tau} \int_{s_-}^{s_+} ds \int_{t_-}^{t_+} dt \frac{1}{2} \sum_{i,f} |\mathcal{M}_{\tau \rightarrow \mu PP}|^2, \quad (\text{C.17})$$

where κ_{PP} is 1 for $PP = \pi^+\pi^-, K^+K^-, K^0\bar{K}^0$ and 1/2 for $PP = \pi^0\pi^0$ (we neglect this one as it vanishes in the charge conjugation symmetry limit). In terms of the momenta of the particles participating in the process, $s = (p_q + p_{\bar{q}})^2$ and $t = (p - p_{\bar{q}})^2$, so that

$$\begin{aligned} t_{\pm}^{\pm} &= \frac{1}{4s} \left[(m_{\tau}^2 - m_{\mu}^2)^2 - \left(\lambda^{1/2}(s, m_{P_1}^2, m_{P_2}^2) \mp \lambda^{1/2}(m_{\tau}^2, s, m_{\mu}^2) \right)^2 \right], \\ s_{-} &= 4m_P^2, \\ s_{+} &= (m_{\tau} - m_{\mu})^2. \end{aligned} \quad (\text{C.18})$$

C.3 $\tau \rightarrow \mu V$

For these cases the branching ratio of $\tau \rightarrow \mu V$ is related with the $\tau \rightarrow \mu PP$ by trying to implement the experimental procedure as follows

$$\text{Br}(\tau \rightarrow \mu V) = \sum_{P_1, P_2} \text{Br}(\tau \rightarrow \mu P_1 P_2) \Big|_V. \quad (\text{C.19})$$

In the above equation the s limits are now restricted to

$$s_{-} = M_V^2 - \frac{1}{2}M_V\Gamma_V, \quad s_{+} = M_V^2 + \frac{1}{2}M_V\Gamma_V. \quad (\text{C.20})$$

Therefore, when $V = \rho, \phi$ their branching ratios are given by

$$\begin{aligned} \text{Br}(\tau \rightarrow \mu \rho) &= \text{Br}(\tau \rightarrow \mu \pi^+ \pi^-) \Big|_{\rho}, \\ \text{Br}(\tau \rightarrow \mu \phi) &= \text{Br}(\tau \rightarrow \mu K^+ K^-) \Big|_{\phi} + \text{Br}(\tau \rightarrow \mu K^0 \bar{K}^0) \Big|_{\phi}. \end{aligned} \quad (\text{C.21})$$

D Appendix: Hadronic form factors

The vector form factors $F_V^{PP}(s)$, defined by eq. (C.14), are based on two key points:

- At $s \ll M_R^2$ (being M_R a generic resonance mass), the vector form factor should match the $\mathcal{O}(p^4)$ result of χ PT [67, 68].
- Form factors of QCD currents should vanish for $s \gg M_R^2$ [76].

We include energy-dependent widths for the wider resonances $\rho(770)$ and $\rho(1450)$ or constant for the narrow ones: $\omega(782)$ and $\phi(1020)$. For the $\rho(770)$ we take the definition put forward in [77]

$$\Gamma_{\rho}(s) = \frac{M_{\rho}s}{96\pi F^2} \left[\sigma_{\pi}^3(s) \theta(s - 4m_{\pi}^2) + \frac{1}{2} \sigma_K^3(s) \theta(s - 4m_K^2) \right], \quad (\text{D.1})$$

where $\sigma_P(s) = \sqrt{1 - 4\frac{m_P^2}{s}}$, while $\rho(1450)$ is parameterized as follows [69]

$$\Gamma_{\rho'}(s) = \Gamma_{\rho'}(M_{\rho'}^2) \frac{s}{M_{\rho'}^2} \left(\frac{\sigma_{\pi}^3(s) + \frac{1}{2} \sigma_K^3(s) \theta(s - 4m_K^2)}{\sigma_{\pi}^3(M_{\rho'}^2) + \frac{1}{2} \sigma_K^3(M_{\rho'}^2) \theta(s - 4m_K^2)} \right) \theta(s - 4m_{\pi}^2), \quad (\text{D.2})$$

with $\Gamma_{\rho'}(M_{\rho'}^2) = 400 \pm 60$ MeV [11]. We get the following expressions for the vector form factors

$$F_V^{\pi\pi}(s) = F(s) \exp \left[2\text{Re} \left(\tilde{H}_{\pi\pi}(s) \right) + \text{Re} \left(\tilde{H}_{KK}(s) \right) \right], \quad (\text{D.3})$$

$$F(s) = \frac{M_\rho^2}{M_\rho^2 - s - iM_\rho\Gamma_\rho(s)} \left[1 + \left(\delta \frac{M_\omega^2}{M_\rho^2} - \gamma \frac{s}{M_\rho^2} \right) \frac{s}{M_\omega^2 - s - iM_\omega\Gamma_\omega} \right] - \frac{\gamma s}{M_{\rho'}^2 - s - iM_{\rho'}\Gamma_{\rho'}(s)}, \quad (\text{D.4})$$

$$\begin{aligned} F_V^{K^+K^-}(s) = & \frac{1}{2} \frac{M_\rho^2}{M_\rho^2 - s - iM_\rho\Gamma_\rho(s)} \exp \left[2\text{Re} \left(\tilde{H}_{\pi\pi}(s) \right) + \text{Re} \left(\tilde{H}_{KK}(s) \right) \right] \\ & + \frac{1}{2} \left[\sin^2 \theta_V \frac{M_\omega^2}{M_\omega^2 - s - iM_\omega\Gamma_\omega} + \cos^2 \theta_V \frac{M_\phi^2}{M_\phi^2 - s - iM_\phi\Gamma_\phi} \right] \exp \left[3\text{Re} \left(\tilde{H}_{KK}(s) \right) \right], \end{aligned} \quad (\text{D.5})$$

$$\begin{aligned} F_V^{K^0\bar{K}^0}(s) = & -\frac{1}{2} \frac{M_\rho^2}{M_\rho^2 - s - iM_\rho\Gamma_\rho(s)} \exp \left[2\text{Re} \left(\tilde{H}_{\pi\pi}(s) \right) + \text{Re} \left(\tilde{H}_{KK}(s) \right) \right] \\ & + \frac{1}{2} \left[\sin^2 \theta_V \frac{M_\omega^2}{M_\omega^2 - s - iM_\omega\Gamma_\omega} + \cos^2 \theta_V \frac{M_\phi^2}{M_\phi^2 - s - iM_\phi\Gamma_\phi} \right] \exp \left[3\text{Re} \left(\tilde{H}_{KK}(s) \right) \right], \end{aligned} \quad (\text{D.6})$$

where we have defined the following terms

$$\begin{aligned} \beta &= \frac{\Theta_{\rho\omega}}{3M_\rho^2}, \\ \gamma &= \frac{F_V G_V}{F^2} (1 + \beta) - 1, \\ \delta &= \frac{F_V G_V}{F^2} - 1, \\ \tilde{H}_{PP}(s) &= \frac{s}{F^2} M_P(s), \\ M_P(s) &= \frac{1}{12} \left(1 - 4 \frac{m_P^2}{s} \right) J_P(s) - \frac{k_P(M_\rho)}{6} + \frac{1}{288\pi^2}, \\ J_P(s) &= \frac{1}{16\pi^2} \left[\sigma_P(s) \ln \frac{\sigma_P(s) - 1}{\sigma_P(s) + 1} + 2 \right], \\ k_P(\mu) &= \frac{1}{32\pi^2} \left(\ln \frac{m_P^2}{\mu^2} + 1 \right). \end{aligned} \quad (\text{D.7})$$

The β parameter includes the contribution of the isospin breaking $\rho - \omega$ mixing through $\Theta_{\rho\omega} = -3.3 \times 10^{-3}$ GeV² [78]. The asymptotic constrain on the $N_C \rightarrow \infty$ vector form factor indicates $F_V G_V \simeq F^2$ [79]. We will use ideal mixing between the octet and singlet vector components, $\theta_V = 35^\circ$. We note that when isospin-breaking effects are turned off, the resummation of the real part of the chiral loop functions is not undertaken and

the contribution from the ρ' is neglected, the well-known results from the vector-meson dominance hypothesis are recovered. More elaborated form factors are obtained using the results presented here as seeds for the input phaseshift in the dispersive formulation, see e.g. refs. [80, 81]. These refinements modify only slightly the numerical results obtained with the form factors quoted in this appendix.

References

- [1] P. W. Higgs, Phys. Rev. Lett. **13** (1964), 508-509.
- [2] P. W. Higgs, Phys. Lett. **12** (1964), 132-133.
- [3] F. Englert and R. Brout, Phys. Rev. Lett. **13** (1964), 321-323.
- [4] G. S. Guralnik, C. R. Hagen and T. W. B. Kibble, Phys. Rev. Lett. **13** (1964), 585-587.
- [5] G. Aad *et al.* [ATLAS], Phys. Lett. B **716** (2012), 1-29.
- [6] S. Chatrchyan *et al.* [CMS], Phys. Lett. B **716** (2012), 30-61.
- [7] H. Georgi, H. R. Quinn and S. Weinberg, Phys. Rev. Lett. **33** (1974), 451-454.
- [8] S. L. Glashow, Nucl. Phys. **22** (1961), 579-588.
- [9] S. Weinberg, Phys. Rev. Lett. **19** (1967), 1264-1266.
- [10] A. Salam, Conf. Proc. C **680519** (1968), 367-377.
- [11] P.A. Zyla, *et al.* (Particle Data Group), Prog. Theor. Exp. Phys. 2020, 083C01 (2020).
- [12] N. Arkani-Hamed, A. G. Cohen, E. Katz and A. E. Nelson, JHEP **07** (2002), 034.
- [13] M. Schmaltz and D. Tucker-Smith, Ann. Rev. Nucl. Part. Sci. **55** (2005), 229-270.
- [14] M. Perelstein, Prog. Part. Nucl. Phys. **58** (2007), 247-291 doi:10.1016/j.pnpnp.2006.04.001 [arXiv:hep-ph/0512128 [hep-ph]].
- [15] G. Panico and A. Wulzer, Lect. Notes Phys. **913** (2016), pp.1-316.
- [16] S. Weinberg, Phys. Rev. D **13** (1976), 974-996.
- [17] N. Arkani-Hamed, A. G. Cohen and H. Georgi, Phys. Rev. Lett. **86** (2001), 4757-4761.
- [18] N. Arkani-Hamed, A. G. Cohen and H. Georgi, Phys. Lett. B **513** (2001), 232-240.
- [19] H. C. Cheng and I. Low, JHEP **09** (2003), 051.
- [20] H. C. Cheng and I. Low, JHEP **08** (2004), 061.
- [21] I. Low, JHEP **10** (2004), 067.
- [22] H. C. Cheng, I. Low and L. T. Wang, Phys. Rev. D **74** (2006), 055001.
- [23] J. Hubisz, P. Meade, A. Noble and M. Perelstein, JHEP **01** (2006), 135.
- [24] J. Hubisz, S. J. Lee and G. Paz, JHEP **06** (2006), 041.
- [25] C. R. Chen, K. Tobe and C. P. Yuan, Phys. Lett. B **640** (2006), 263-271.
- [26] M. Blanke, A. J. Buras, A. Poschenrieder, C. Tarantino, S. Uhlig and A. Weiler, JHEP **12** (2006), 003.
- [27] A. J. Buras, A. Poschenrieder, S. Uhlig and W. A. Bardeen, JHEP **11** (2006), 062.
- [28] A. Belyaev, C. R. Chen, K. Tobe and C. P. Yuan, Phys. Rev. D **74** (2006), 115020.
- [29] M. Blanke, A. J. Buras, A. Poschenrieder, S. Recksiegel, C. Tarantino, S. Uhlig and A. Weiler, JHEP **01** (2007), 066.
- [30] C. T. Hill and R. J. Hill, Phys. Rev. D **76** (2007), 115014.
- [31] T. Goto, Y. Okada and Y. Yamamoto, Phys. Lett. B **670** (2009), 378-382.

- [32] M. Blanke, A. J. Buras, B. Duling, S. Recksiegel and C. Tarantino, *Acta Phys. Polon. B* **41** (2010), 657-683.
- [33] X. F. Han, L. Wang, J. M. Yang and J. Zhu, *Phys. Rev. D* **87** (2013) no.5, 055004.
- [34] B. Yang, N. Liu and J. Han, *Phys. Rev. D* **89** (2014) no.3, 034020.
- [35] J. Reuter, M. Tonini and M. de Vries, *JHEP* **02** (2014), 053.
- [36] B. Yang, G. Mi and N. Liu, *JHEP* **10** (2014), 047.
- [37] M. Blanke, A. J. Buras and S. Recksiegel, *Eur. Phys. J. C* **76** (2016) no.4, 182.
- [38] D. Dercks, G. Moortgat-Pick, J. Reuter and S. Y. Shim, *JHEP* **05** (2018), 049.
- [39] J. I. Illana and J. M. Pérez-Poyatos, *Eur. Phys. J. Plus* **137** (2022) no.1, 42.
- [40] M. Blanke, A. J. Buras, B. Duling, A. Poschenrieder and C. Tarantino, *JHEP* **05** (2007), 013.
- [41] F. del Aguila, J. I. Illana and M. D. Jenkins, *JHEP* **01** (2009), 080.
- [42] F. del Aguila, J. I. Illana and M. D. Jenkins, *JHEP* **09** (2010), 040.
- [43] T. Goto, Y. Okada and Y. Yamamoto, *Phys. Rev. D* **83** (2011), 053011.
- [44] W. Liu, C. X. Yue and J. Zhang, *Eur. Phys. J. C* **68** (2010), 197-207.
- [45] W. Ma, C. X. Yue, J. Zhang and Y. B. Sun, *Phys. Rev. D* **82** (2010), 095010.
- [46] J. Z. Han, X. L. Wang and B. F. Yang, *Nucl. Phys. B* **843** (2011), 383-395.
- [47] T. Goto, R. Kitano and S. Mori, *Phys. Rev. D* **92** (2015), 075021.
- [48] B. Yang, J. Han and N. Liu, *Phys. Rev. D* **95** (2017) no.3, 035010.
- [49] F. del Aguila, L. Ametller, J. I. Illana, J. Santiago, P. Talavera and R. Vega-Morales, *JHEP* **08** (2017), 028 [erratum: *JHEP* **02** (2019), 047].
- [50] F. del Aguila, L. Ametller, J. I. Illana, J. Santiago, P. Talavera and R. Vega-Morales, *JHEP* **07** (2019), 154.
- [51] F. Del Aguila, J. I. Illana, J. M. Perez-Poyatos and J. Santiago, *JHEP* **12** (2019), 154.
- [52] Iván Pacheco and Pablo Roig, *JHEP* **02** (2022), 054.
- [53] A. Lami, J. Portolés, P. Roig, *Phys. Rev. D* **93**, 076008 (2016),
- [54] Monika Blanke, *et al.*, *JHEP* **01** (2007), 066.
- [55] Francisco del Aguila, *et al.*, *JHEP* **12**, (2019), 154.
- [56] Jay Hubisz, *et al.*, *JHEP* **06**, (2006), 041.
- [57] Jay Hubisz and Patrick Meade, *Phys.Rev. D* **71** (2005) 035016.
- [58] Ian Low, *JHEP* **10** (2004), 067.
- [59] J. de Blas, Effective Lagrangian Description of Physics Beyond the Standard Model and Electroweak Precision Tests, Ph.D. Thesis, Granada 2010.
- [60] A. Celis, V. Cirigliano and E. Passemar, *Phys. Rev. D* **89** (2014), 013008.
- [61] A. Celis, V. Cirigliano and E. Passemar, *Phys. Rev. D* **89** (2014) no.9, 095014.
- [62] T. Husek, K. Monsálvez-Pozo and J. Portolés, *JHEP* **01** (2021), 059.
- [63] V. Cirigliano, K. Fuyuto, C. Lee, E. Mereghetti and B. Yan, *JHEP* **03** (2021), 256.

- [64] G. Hernández-Tomé, *et al.*, Phys. Rev. D **101**, (2020) 075020.
- [65] G. Ecker, J. Gasser, A. Pich and E. de Rafael, Nucl. Phys. B **321** (1989), 311-342.
- [66] G. Ecker, J. Gasser, H. Leutwyler, A. Pich and E. de Rafael, Phys. Lett. B **223** (1989), 425-432.
- [67] J. Gasser and H. Leutwyler, Annals Phys. **158** (1984), 142.
- [68] J. Gasser and H. Leutwyler, Nucl. Phys. B **250** (1985), 465-516.
- [69] E. Arganda, M. J. Herrero and J. Portolés, JHEP **06** (2008), 079.
- [70] R. Escribano, S. Gonzalez-Solís and P. Roig, Phys. Rev. D **94** (2016) no.3, 034008.
- [71] R. Kaiser and H. Leutwyler, Eur. Phys. J. C **17** (2000), 623-649.
- [72] P. Roig, A. Guevara and G. López Castro, Phys. Rev. D **89** (2014) no.7, 073016.
- [73] A. Guevara, P. Roig and J. J. Sanz-Cillero, JHEP **06** (2018), 160.
- [74] Francisco del Aguila, *et al.*, JHEP **08**, (2017) 028.
- [75] M. A. Arroyo-Ureña, R. Gaitán and T. A. Valencia-Pérez, “**SpaceMath** version 1.0. A **Mathematica** package for beyond the standard model parameter space searches,” [arXiv:2008.00564 [hep-ph]].
- [76] G. P. Lepage and S. J. Brodsky, Phys. Rev. D **22** (1980), 2157.
- [77] D. Gomez Dumm, A. Pich and J. Portoles, Phys. Rev. D **62** (2000), 054014 doi:10.1103/PhysRevD.62.054014 [arXiv:hep-ph/0003320 [hep-ph]].
- [78] A. Pich and J. Portolés, Nucl. Phys. Proc. Suppl. **121** (2003) 179.
- [79] G. Ecker, J. Gasser, H. Leutwyler, A. Pich and E. de Rafael, Phys. Lett. B **223** (1989) 425; F. Guerrero and A. Pich, Phys. Lett. B **412** (1997) 382.
- [80] D. Gómez Dumm and P. Roig, Eur. Phys. J. C **73** (2013) no.8, 2528.
- [81] S. González-Solís and P. Roig, Eur. Phys. J. C **79** (2019) no.5, 436.